Mixed carbonate-siliciclastic tidal sedimentation in the Miocene to Pliocene Bouse Formation, palaeo-Gulf of California

Brennan O'Connell[1,3], Rebecca J. Dorsey[1], Stephen T. Hasiotis[2], Ashleigh v.s. Hood[3]

[1]Department of Earth Sciences, University of Oregon, Eugene, OR, United States
[2]Department of Geology, University of Kansas, Lawrence, KS, USA
[3]current, School of Earth Sciences, University of Melbourne, Parkville, Victoria 3051, Australia

Post Print October 2020 *Sedimentology* DOI: 10.1111/sed.12817

Mixed carbonate-siliciclastic tidal sedimentation in the Miocene to Pliocene Bouse Formation, palaeo-Gulf of California

Brennan O'Connell[1,3], Rebecca J. Dorsey[1], Stephen T. Hasiotis[2], Ashleigh v.s. Hood[3]

[1]Department of Earth Sciences, University of Oregon, Eugene, OR, United States
[2]Department of Geology, University of Kansas, Lawrence, KS, USA
[3]current, School of Earth Sciences, University of Melbourne, Parkville, Victoria 3051, Australia

Keyword: Colorado River, rhythmites, tidal strait, fluvial-tidal, trace fossils, *Thalassinoides*

Post Print October 2020 *Sedimentology* DOI: 10.1111/sed.12817

ABSTRACT

Mixed carbonate-siliciclastic deposits provide unique insights into hydrodynamic processes that control sedimentation in tidal systems. This study presents sedimentologic and ichnologic data from the upper Miocene to lower Pliocene Bouse Formation, which accumulated during regional transgression at the margin of a tidal strait near the north end of the ancestral Gulf of California. The basal carbonate member of the Bouse Formation records deposition in a tide-influenced, compositionally mixed carbonate-siliciclastic system dominated by salt marsh, tidal flat, and channel environments. The basal carbonate member is an overall deepening up succession of facies associations (FA) comprising: FA1 siliciclastic-rich heterolithic facies, lime mudstone with desiccation cracks, and plant debris rich carbonate silt interpreted as siliciclastic-rich tidal flats; FA2 well-sorted gravels, siliciclastic-rich sandy strata, lime mudstone with desiccation cracks, and sandy microbial micrite interpreted as tidal-channel deposits; FA3 carbonate-rich heterolithic lime mudstone to well sorted, crossbedded bioclastic grainstone interpreted as intertidal to shallow subtidal deposits; and FA4 lime mudstone interpreted as shallow to deep subtidal low-energy deposits that record the end of tidal conditions in the basin. Trace fossils include marine forms *Gyrolithes, Teichichnus, Thalassinoides,* and non-diagnostic forms *Arenicolites*, *Cochlichnus, Conichnus*, *Lockeia*, *Planolites*, *Skolithos,* and *Treptichnus* (known from marine, brackish, and freshwater environments). The diminutive size of trace fossils reflects brackish conditions created by mixing of freshwater and seawater. This study provides evidence for a late Miocene to early Pliocene humid climate in southwestern North America, in stark contrast to the modern hyperarid climate. Factors that controlled the relative percent of mixed carbonate and siliciclastic sediment include siliciclastic input from local rivers, *in situ* carbonate production, current energy, degree of tidal mixing, and relative sea level. Pronounced facies variability at bedform, outcrop, and basin

scale documented in this study appears to be an important characteristic of mixed carbonate-siliciclastic deposits in tidal depositional systems.

INTRODUCTION

Mixed carbonate-siliciclastic sediments are common in the geological record and reflect interactions between climate, siliciclastic input, tectonics, basin geometry, transport process, and oceanographic conditions (e.g., Mount et al., 1984; Pilkey et al., 1988; Dolan, 1989; Dorsey & Kidwell, 1999; Chiarella et al., 2017). Mixed-composition deposits offer a sensitive record of hydrodynamic processes and conditions compared to their pure carbonate or siliciclastic counterparts because of the unique physical properties of carbonate and siliciclastic grains (e.g., Breda & Preto, 2011; Longhitano, 2011; Chiarella et al., 2017). Mixed carbonate-siliciclastic sediments are also important for hydrocarbon exploration because they are characterised by strong contrasts in permeability and porosity that may influence flow migration and reservoir properties (e.g., McNeill, 2004; Ainsworth, 2010; Chiarella et al., 2017). Despite their significance, mixed carbonate-siliciclastic deposits in the stratigraphic record remain relatively under studied.

A general understanding of mixed carbonate-siliciclastic sedimentation is derived from early work that highlighted classification schemes, styles of mixing, and the role of sea-level change in marine shelf settings (e.g., Zuffa, 1980; Mount, 1984, 1985). The traditional view is that siliciclastic input to marine shelf environments occurs during relative sea-level lowstand, and carbonates are preferentially deposited during highstand when siliciclastic sediment is trapped in estuaries and rivers (e.g., Van Siclen, 1958; Wilson, 1967). Lowstand deposition of carbonate and highstand deposition of sandstone, however, can occur (Brachert et al., 2003), and relative sea-level change is just one of several factors that can act alone or in combination with other processes to control sedimentation in tidal settings. For example, fluvial input of siliciclastic sediment to the Great Barrier Reef is strongly controlled by changes in precipitation, and complex physical mixing of carbonate and siliciclastic sediment often results from base-level changes (e.g., Page & Dickens, 2005). Fluvial input, source mixing, and aeolian input can also contribute to mixing of carbonate and siliciclastic sediment (e.g., Piller & Mansour, 1994). Tidal and wind currents may circulate siliciclastic sediment that dilutes but does not completely shut off carbonate precipitation (e.g., Zeller et al., 2015). In addition, tectonically controlled changes in palaeoceanographic circulation can result in variable stacking patterns and mixed sediment composition along the shoreline (Chiarella et al., 2019). These are just a few examples of the processes and factors that control mixed carbonate and siliciclastic deposition in modern and ancient settings.

Recent studies have documented mixed carbonate siliciclastic sediments from microtidal, mixed carbonate siliciclastic deposits of Neogene–Pleistocene tidal bay-fill successions and confined straits of southern Italy, Mediterranean Sea (e.g., Di Stefano & Longhitano, 2009; Longhitano et al., 2010, 2012a, 2014; Chiarella et al., 2012, 2019; Chiarella & Longhitano, 2012). The Mediterranean studies are especially insightful because ancient deposits are exposed adjacent to their modern equivalents, allowing researchers to constrain sedimentary processes and stratal geometries in tidal straits and basins. These studies have advanced understanding of deposition in mixed carbonate-siliciclastic microtidal settings, but mixed sedimentation in other types of tidal systems is less well understood. Additional work is needed in areas where interpretation of ancient successions is provided by proximity to comparable modern environments in various tidal settings. Variable parameters of interest include carbonate assemblage type, tidal range, climate, tectonics, amount and type of detrital sediment input, and basin geometry.

The northern Gulf of California region is an excellent natural laboratory to study tidal depositional systems because ancient deposits are exposed close to modern macrotidal flats that provide unique insights into depositional processes and products (Thompson, 1975). The focus of this study is the upper Miocene to lower Pliocene Bouse Formation in its southern exposures along the lower Colorado River region, which accumulated at the margin of a tidal strait near the north end of the ancestral Gulf of California (Fig. 1; O'Connell et al., 2017; Dorsey et al., 2018; Garnder & Dorsey, in press). The basal carbonate member of the Bouse Formation is characterised by compositional mixing (*sensu* Chiarella et al., 2017), reflecting contemporaneous accumulation of carbonate and siliciclastic sediment at laminae and bed scales (Chiarella et al., 2017). The Bouse Formation deposits display tidal cyclicity similar to that of the modern Gulf of California (Marinone, 1997; O'Connell et al., 2017), and the tectonic setting and basin geometries are well constrained (Dorsey et al., 2018; Garnder & Dorsey, in press). Published analyses, however, are incomplete, and some studies favour a lacustrine origin for the Bouse Formation in its southern exposures along the lower Colorado River region (e.g., Spencer & Patchett, 1997; House et al., 2008; Spencer et al., 2013; Bright et al., 2016, 2018a, 2018b).

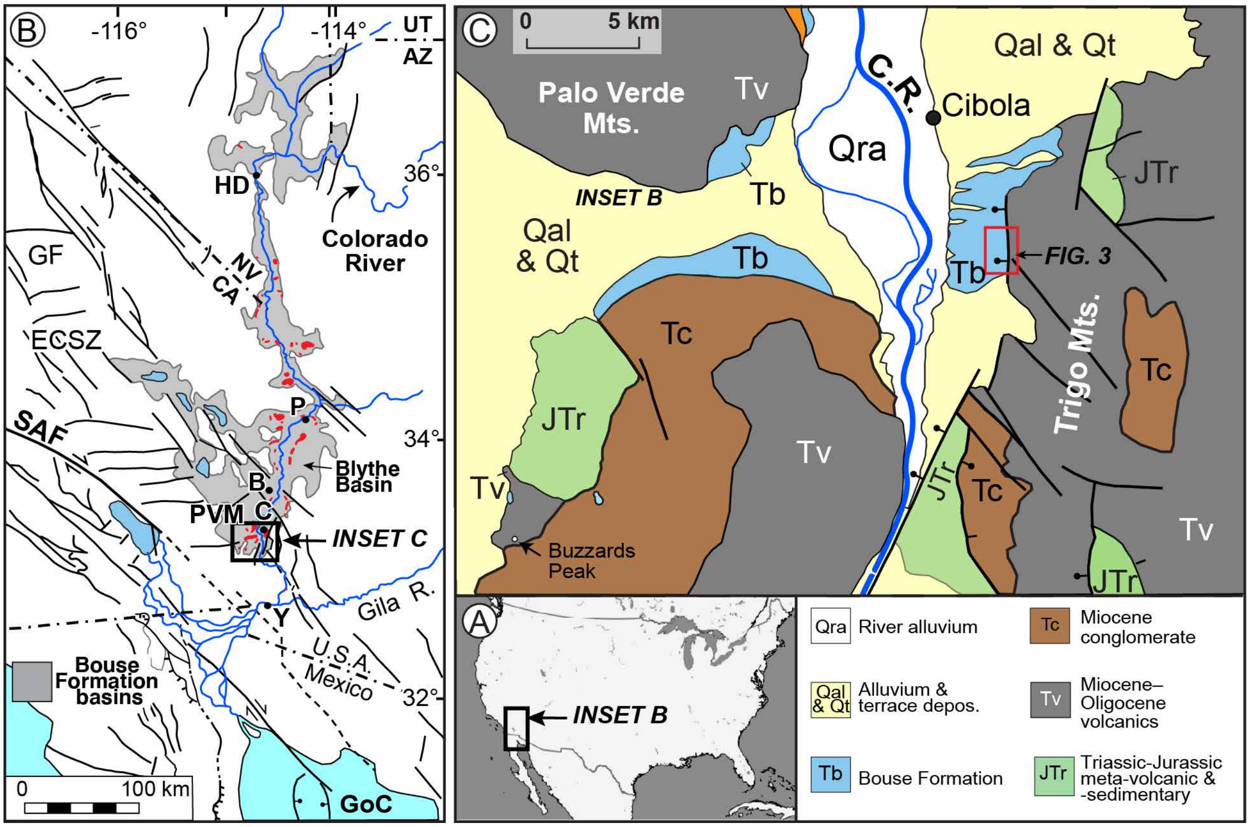

Figure 1. A. Map of USA. B. Map of lower Colorado River region showing major faults, exposures of Bouse Formation (Fm.) (red), and Bouse Formation depositional basins of Spencer et al. (2008) (grey). Abbreviations: B, Blythe; C, Cibola; HD, Hoover Dam; P, Parker; SAF, San Andreas fault; ST, Salton Trough; Y, Yuma; GF, Garlock Fault; ECSZ, Eastern California Shear Zone; GoC, Gulf of California. C. Simplified geologic map of study area (compiled from Sherrod and Tosdal, 1991; Richard, 1993). C.R., Colorado River. Modified from O'Connell et al., (2017).

This paper presents an integrated sedimentologic, ichnologic, petrographic, and palaeoclimatic analysis that sheds new insight into the depositional processes, environments, and climatic setting of the basal carbonate member of the Bouse Formation in its southern exposures. Facies associations documented in this study formed on the low gradient eastern margin of the Blythe basin, in contrast to age-equivalent facies that accumulated on the steeper west margin of the basin in the southeastern Palo Verde Mountains (Fig. 1; Garnder & Dorsey, in press). Different facies models, therefore, are required despite the proximity of deposits. This study includes a systematic, detailed facies analysis to establish the setting and depositional environments for the ~5.0–6.5 Ma northern Gulf of California. Data are then compared to the present day Gulf of California where tidal cyclicity, tidal range, and depositional facies are known (e.g., Thompson, 1975; Halfar et al., 2004), providing an excellent modern analogue for tidal currents and processes. This study advances an understanding of mixed carbonate-siliciclastic settings in general, and provides a facies model to aid in recognising similar settings in the geological record.

REGIONAL GEOLOGY

The Bouse Formation is a widespread, upper Miocene to lower Pliocene succession of carbonate and siliciclastic deposits exposed discontinuously along the lower Colorado River corridor (Figs. 1, 2). The study area is located southeast of Cibola, Arizona, at the eastern margin of the southern Blythe basin (Figs. 1, 3), where prior geologic mapping established the distribution and relative age relations of Miocene to Quaternary deposits (Homan, 2014; Gootee et al., 2016). The Bouse Formation in the studied area formed at the margin of a tidal strait near the north end of the Gulf of California oblique rift as indicated by marine and brackish-water fossils and a wide range of tidal sedimentary structures (e.g., Buising, 1990; Turak, 2000; McDougall, 2008; McDougall & Miranda-Martinez, 2014; O'Connell et. al., 2017; Dorsey et al., 2018; Garnder & Dorsey, in press). Although some authors favour an isolated inland-lake model for the Bouse Formation in the study area (Spencer & Patchett, 1997; House et al., 2008; Spencer et al., 2008, 2013; Bright et al., 2016, 2018a; 2018b), the lacustrine model is incompatible with abundant evidence for intertidal, marine to brackish-water fossils and trace fossils, and widespread tide-influenced sedimentary structures (Buising, 1990; Turak, 2000; O'Connell et al., 2017; Dorsey et al., 2018; Garnder & Dorsey, in press).

The Bouse Formation in the study area is divided into three laterally persistent members: basal carbonate member, siliciclastic member, and upper bioclastic member (Dorsey et al., 2018). The Bouse Formation rests unconformably on Miocene alluvial-fan conglomerate consisting of poorly sorted sandy conglomerate and pebbly sandstone with clasts of volcanic, intrusive, and metamorphic rocks (Fig. 2), representing pre late Miocene basin fill that accumulated in extensional and transtensional basins prior to late Miocene marine incursion and deposition of the Bouse Formation (e.g., Buising, 1990; Sherrod & Tosdal, 1991; Richard, 1993; House et al., 2008; Spencer et al., 2008, 2013; Homan, 2014).

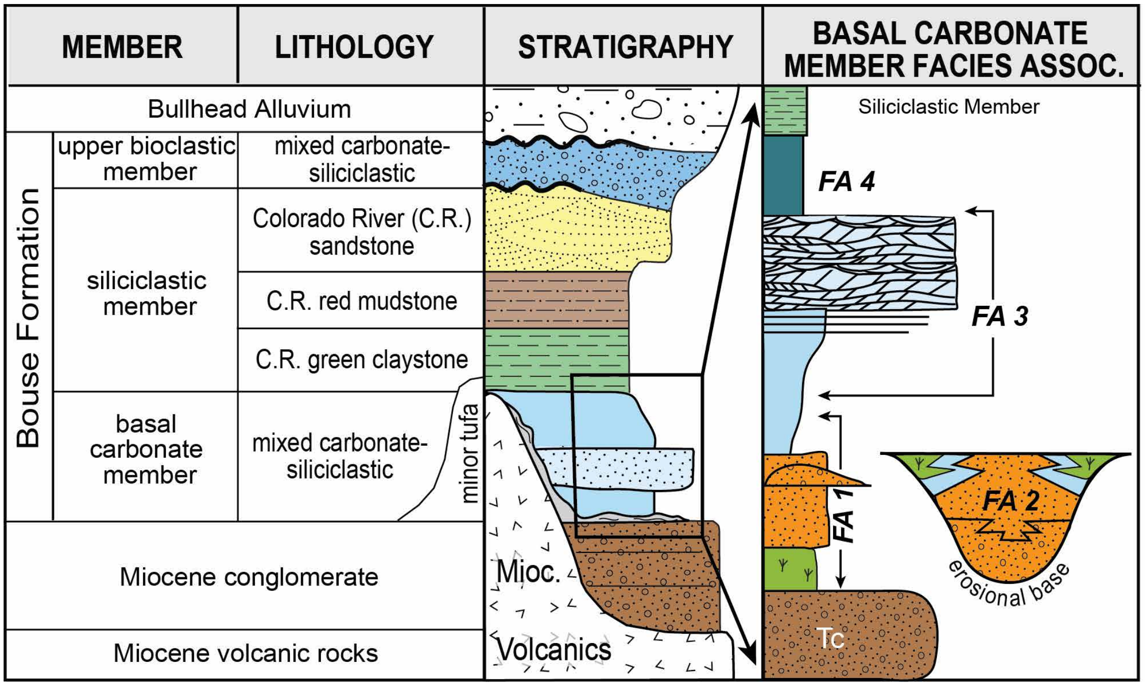

Figure 2. Representative members, lithology, and stratigraphy of southern exposures of Bouse Formation along the lower Colorado River. Modified from Homan (2014) and Dorsey et al. (2018). Tc, Miocene conglomerate; FA, Facies association.

The basal carbonate member of the Bouse Formation ranges from ~0.5 to 15 m thick and includes: (1) rare bedrock-encrusting travertine and tufa that records the first arrival of carbonate-oversaturated waters fed by deeply-sourced groundwater and carbonate-oversaturated freshwater (Crossey et al., 2015, 2017); (2) mixed carbonate-siliciclastic deposits; and (3) and upper lime mudstone (Fig. 2). This study focuses on mixed carbonate-siliciclastic facies and lime mudstone facies exposed on the east side of the Blythe basin (Figs. 1, 2, 3). In the SE Palo Verde Mountains west of the Colorado River (Fig. 1C), the basal carbonate member contains an age-equivalent suite of facies that record marine transgression of a steep rocky shoreline followed by subtidal deposition of coarse bioclastic dunes in a high-energy tidal strait (Garnder & Dorsey, in press).

The siliciclastic member of the Bouse Formation conformably but sharply overlies the basal carbonate member, and displays thickness ranging from 0 m at basin margins to 200 m in the subsurface (Metzger et al., 1973). The siliciclastic member is comprised of Colorado River-derived claystone, siltstone, and crossbedded deltaic and river channel sandstone, and records the first arrival of Colorado River sediment (Fig. 2; Homan, 2014; Dorsey et al., 2018). The upper bioclastic member unconformably overlies the lower two members and consists of water-lain, mixed carbonate-siliciclastic calcarenite, pebbly calcarenite, and calcareous-matrix conglomerate (Fig. 2; Homan, 2014; Dorsey et al., 2018). The Bullhead Alluvium and younger Quaternary terrace gravels erosionally overlie the Bouse Formation (Fig. 2; House et al., 2008; Howard et al., 2015).

METHODS

Fourteen stratigraphic sections—including two detailed sections with ichnofossil data (Fig. 4)—were selected as representative examples from measured sections in the study area (see O'Connell, 2016). Stratigraphic sections were measured in exposed cut banks of desert washes (Fig. 3) at the cm- to m-scale using a Jacob's staff. All stratigraphic sections begin at the wash bottom and end at the top of exposed beds—either the top of the Bouse Formation or the top of erosionally inset younger Quaternary terrace gravels. Stratigraphic sections were measured generally 50–200 m apart, depending on outcrop accessibility and stratigraphic completeness.

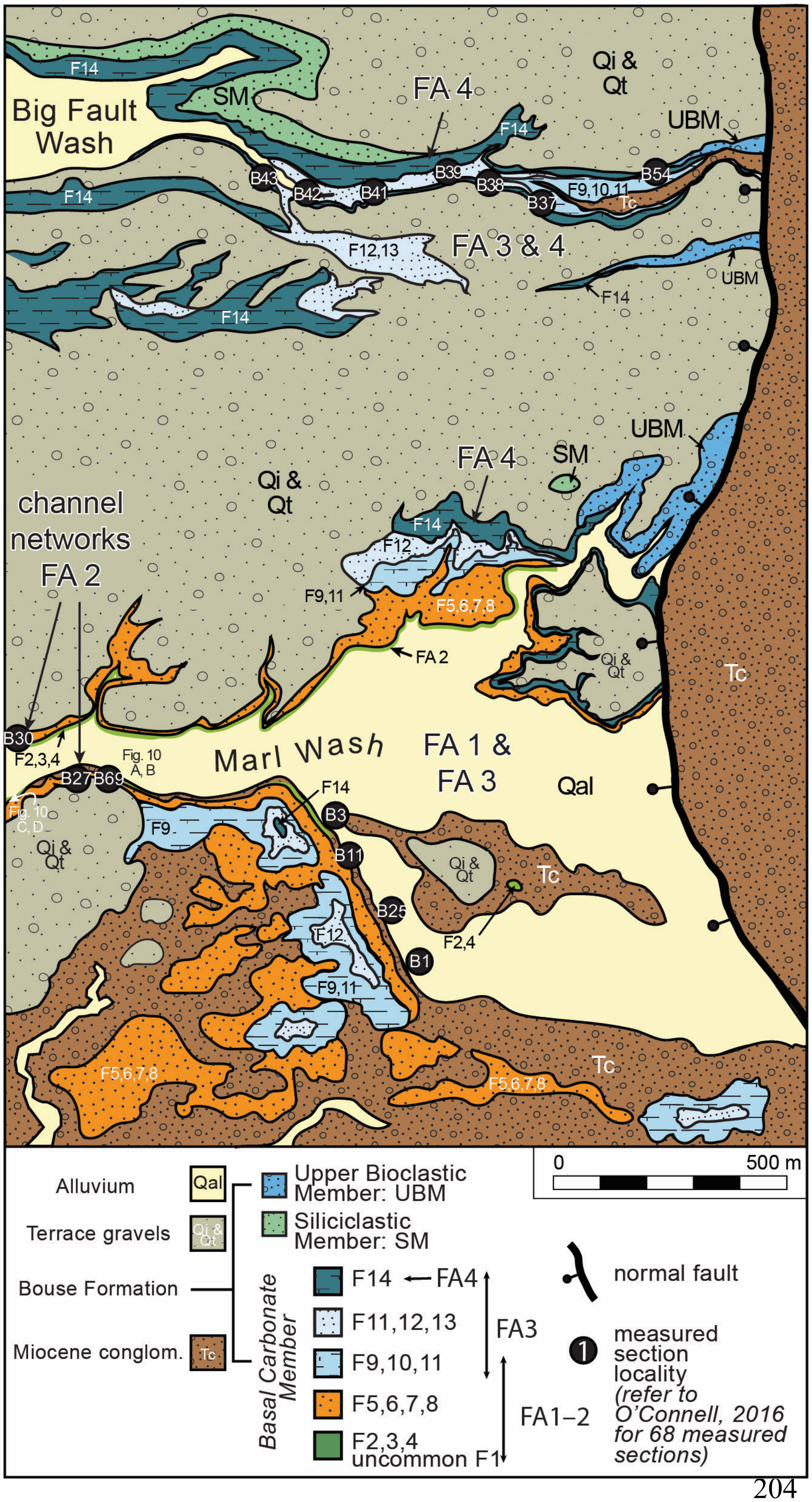

Figure 3. Detailed geologic map of study locations south of Cibola, AZ. Modified from Gootee et al., 2016. See Fig. 1 for regional view.

Data collected include lithology and texture (grain size and sediment sorting), bed thickness and bed geometry at the bedform and outcrop scale, sedimentary structures, and ichnofossils. Palaeocurrent measurements were taken where three-dimensional (3D) surfaces were exposed and accessible. The bioclastic/siliciclastic ratio (b/s) and segregation index (SI) are used to document the carbonate-siliciclastic percentages and the degree of segregation of particles (*sensu* Chiarella & Longhitano, 2012). Sediment was considered unmixed if the antithetic component was < 10% (Mount, 1985; Chiarella & Longhitano, 2012). Measured sections were correlated in the field using such key stratigraphic surfaces as *Thalassinoides*-bearing beds, well-cemented beds, or the base of the lime mudstone facies sharply overlying tidal deposits. These key contacts were walked out to document lateral facies transitions. Trace fossils were identified by their architectural and surficial morphologies and fill type (Hasiotis & Mitchell, 1993; Bromley, 1996). Samples were collected within measured sections and in laterally equivalent beds. Representative samples were taken for thin section petrographic analysis.

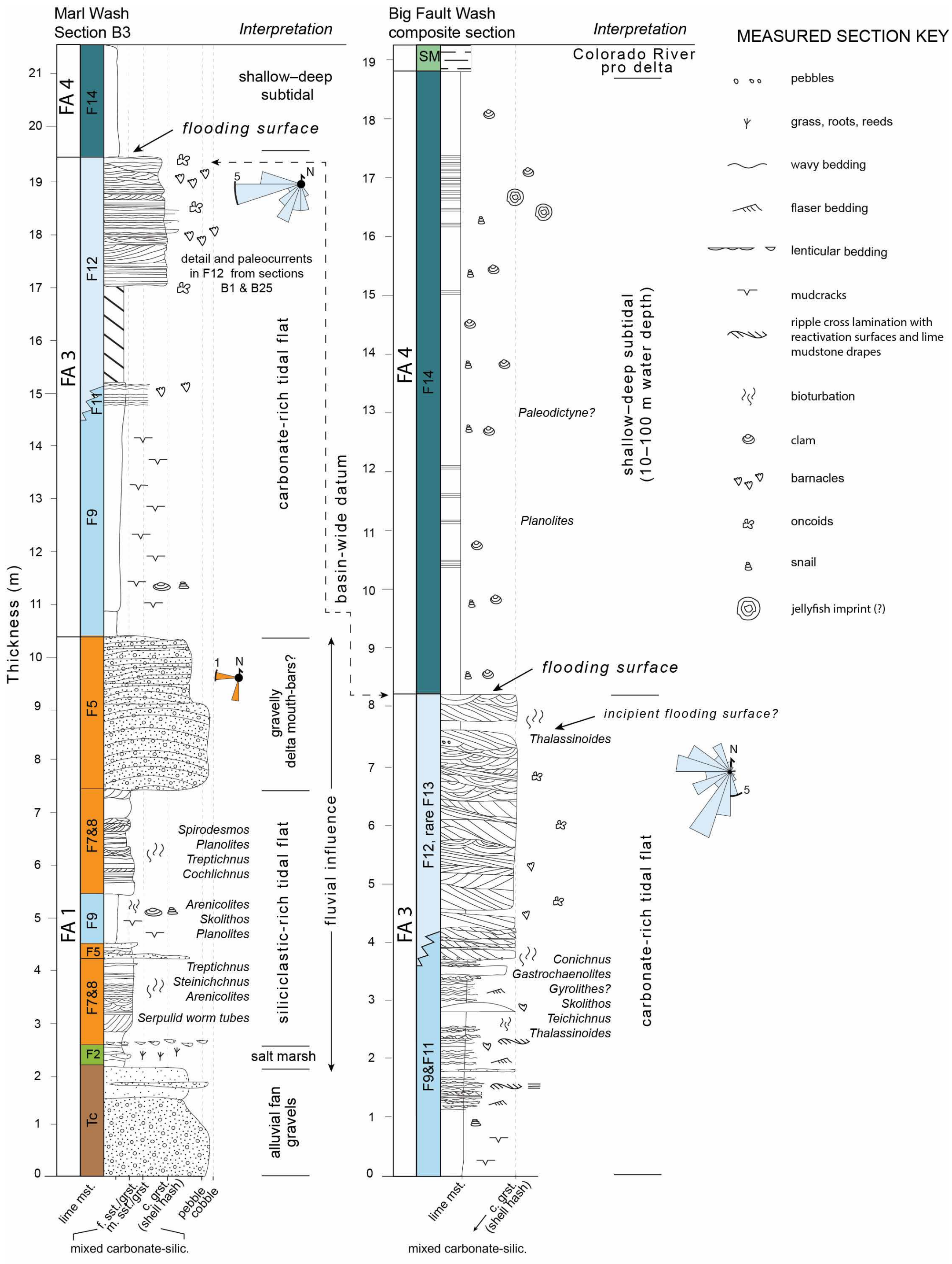

Figure 4. Detailed stratigraphic sections from Marl Wash and Big Fault Wash localities (see Fig. 3). FA, Facies Association; F, Facies (see Table 1); Tc, Miocene conglomerate.

FACIES ASSOCIATIONS

This study documents 14 facies (Table 1) that are identified based on lithology and texture (grain size and sediment sorting), bed thickness, geometry at the bedform and outcrop scale, sedimentary structures, fossil content and ichnofossil data, and the degree of bioclastic-siliciclastic mixing (b/s) (*sensu* Chiarella & Longhitano, 2012). A detailed description of facies is provided in Table 1. From these 14 facies (F), four facies associations (FA) (Fig. 2; Table 2) are recognised and described in detail. Facies associations were grouped based on the common and predictable occurrence of facies in the stratigraphy, as well as such lateral and vertical facies relationships as common interbedding or lateral equivalence. Facies associations are described in their typical stratigraphic order from the base to the top of the basal carbonate member. Facies associations 1–4 are present in the Marl Wash area, and FA3–FA4 with minor FA1 are present in Big Fault Wash (Fig. 3). This analysis excludes a distinctive freshwater tufa and travertine unit at the base of the basal carbonate member of the Bouse Formation elsewhere (e.g., Palo Verde Mountains; Crossey et al., 2017; Dorsey et al., 2018) but is absent in the area south of Cibola, Arizona, where this study is focused (Figs. 1C; 3).

Facies Association 1 (FA1): Siliciclastic-rich tidal flats

Sedimentology: This facies association (Table 2; Figs. 4–7) includes the following facies: cobble lag (F1), matted plant debris rich carbonate silt (F2), thinly bedded poorly sorted conglomerate (F4), crossbedded well-sorted conglomerate (F5), crossbedded sandstone (F6), ripple-laminated calcareous sandstone (F7), heterolithic bedding (F8), and lime mudstone with desiccation cracks (F9) (Tables 1, 2). This association is dominated by compositionally mixed (carbonate-siliciclastic) strata. The carbonate-siliciclastic fraction is generally ~50:50 (b/s = 1) (F2, F6, F7 F8), although the siliciclastic fraction can be ~70% (b/s < 1) (F4, F7) or can exceed 90% (b/s<<1) (F1, F5, rare F6 and F7). The siliciclastic fraction drops to ~10% (b/s >> 1) or unmixed in some carbonate-rich heterolithic beds of F8 and F9.

These facies are grouped together because they are closely interbedded and laterally equivalent deposits (Figs. 4, 5). Centimetre- and m-scale interbedding is common in these deposits, as are lateral facies changes over the m-scale. For example, the base of FA 1 is generally interbedded plant debris rich facies (F2) and conglomerate (F4) (and rare F1) (Figs. 4, 5). These facies are overlain by interbedded flat-based, well-sorted gravels (F5), well-sorted sandy (F7), and

TABLE 1. Bouse Formation basal carbonate member facies

Facies Name	Facies #	Lithofacies description	Sedimentary structures	Ichnology/ fossil content/ plant material	Bed thickness	Typical b/s ratio	Sedimentary process	Interpretation of depositional environment
Cobble lag	1	Well sorted locally derived volcaniclastic cobbles distributed as a single-clast horizon at the base of the basal carbonate member. Lack of fine-grained sediment. Occasional rounded and reworked carbonate clasts. Rare facies in Marl Wash and Big Fault Wash.			15–20 cm	unmixed (siliciclastic)	Winnowing, reworking, and concentrating cobble clasts derived from Miocene alluvial-fan conglomerate and earliest Bouse carbonates.	Conglomerate possibly associated with a sequence boundary; F1 at base of FA2 is a gravelly channel lag.
Matted plant debris rich carbonate silt	2	Thin beds of matted mixed carbonate-siliciclastic silt drape underlying strata. Extremely rare gypsum pseudomorphs. Some beds recessive, poorly-sorted, weakly laminated to massive carbonate-sandy lime mudstone.	Wavy bedding; pinch-and -swell along bedding planes	Abundant carbonate plant debris material (grasses, reed casts, root casts) (Figs. 6E,7B)	0.1–2 cm	b/s=1	Deposition from occasional flooding, baffling, and sediment entrapment in highly-vegetated marshes; rooting; exposure; rare evaporite mineral formation.	Supratidal salt marsh; extrememly rare evaporite mineral formation may indicate deposition in a humid climate.
Sandy microbial micrite	3	Mixed composition silicified sandy microbial micrite. Siliciclastic portion can exceed 50%. Commonly found along the margins of channel deposits (FA2). Weathers into well-cemented large slabs.	Irregular laminations; can be massive	Vertebrate tracks include felines, horses, elephants, and camels; charophytes (Sarjeant et al., 2002; Sarjeant & Reynolds 2001; Metzger, 1968	< 7 cm	b/s=1		Upper intertidal to supratidal algal marsh along the margins of channels (FA2).
Thinly bedded poorly sorted conglom.	4	Locally includes ~7- to 10-cm thick beds of poorly sorted locally-derived granular sandy conglomerate with sharp erosional bases and tops. Carbonate and siliciclastic-rich matrix. Clasts angular to sub-rounded, with matrix-supported pebbles concentrated at base. Associated with F2.	No imbrication		~7–10-cm	b/s<1 to unmixed (siliciclastic)		Pebbly gravel beds may represent accumulation at the base of small runoff-channels in this local catchment, or tidal creek deposits.
Crossbedded well-sorted conglom.	5	Golden brown to gray green, rounded to subrounded, well-sorted to extremely well-sorted, coarse siliciclastic sandstone and pebble-cobble conglomerate. Systematic up slope and down slope variations in grain size occur in foresets. These deposits are often discontinuous laterally, exhibiting strongly lenticular geometry. Sometimes domed or planar geometries (Fig. 6A). Primary dips ranging from nearly horizontal to steep foresets (~20–30°). Gravels can have a lack of fine-grained matrix material (open-networks). Interbeds of carbonate-rich sand are locally present. Clasts consist primarily of granitic and intermediate plutonic, volcanic breccia, and unwelded volcanic tuff. If present, matrix is mixed carbonate and siliciclastic sand. Pebble beds, 1–3 granule to small pebble grains thick, can extend laterally from toe of lenticular cross-bedded gravel foresets.	Inverse, normally graded, and ungraded beds.		Tabular cross stratified-crossbed sets 0.5–3 m; pebble beds 1–3 cm	b/s<1 to unmixed (siliciclastic)	Sediment delivered by small local catchments and transported, reworked, and deposited by migrating gravelly bedforms.	These gravels likely represent a range of bedforms and are typically found at the base of channel fill (FA2) and as gravelly bedforms in relatively siliciclastic tidal flat deposits (FA1). Some gravel bedforms may represent channel fill, barchan dunes, delta mouth bars and/or gilbert deltas. Additional work is needed to understand all conglomerate depositional environments.
Crossbedded sst	6	Golden brown to gray green, well-sorted fine-medium grained siliciclastic sandstone. Comprised of same grain-type lithologies as F5. Associated with minor barnacle and oncoid packstone. Siliciclastic component >95%. Limited to one basin-margin locality in Big Fault Wash.	Trough crossbedding		50 cm	b/s=1 to unmixed (siliciclastic)	Likely deposited by unidirectional currents, although limited 2D outcrop does not allow for accurate paleocurrent measurements.	Small catchment at interface of marine environments?
Ripple-lam. calcareous sst	7	Sandy calcarenite and calcarenitic sandstone: fine- to medium- grained, laminated to thick bedded, admixed carbonate and siliciclastic sandstone (Fig. 6, 7). Siliciclastic component generally ranges from 30% to 70% in the siliciclastic-carbonate mixture (commonly ~50%, although rarely siliciclastic component can exceed ~90%).	Ripple cross lamination, trough and tabular cross-bed sets, parallel lamination, dessication cracks, unidirectional, massive beds; climbing and combined flow ripples	Rare horse tracks, *Serpulid* worm tubes, escape burrows assoc. with unidirectional ripples *Arenicolites, Cochlichnus, Planolites, Spiroesmos, Skolithos, Steinichchnus, Treptichnus, Thalassinoides*	Beds 20–80 cm (FA1); Cross-strata up to 2.8 m (FA2)	b/s=1 to b/s<1	Deposition by tidal bars and dunes; systematic hydraulic sorting of carbonate and siliciclastic sediment by tidal currents.	Tidal bars and dunes on mixed relatively siliciclastic-rich lower tidal flats (FA1). Some sandy bedforms comprise channel fill (FA2). Fluvial influence.
Heterolithic bedding (silici.-rich)	8	Admixed, well-sorted sandy calcarenite, calcarenitic sandstone, and lime mudstone. Recessive (Fig. 7 C,D).	Wavy, flaser, and lenticular bedding	Similar assemblage to F7	0.2–1.5 m	b/s=1	Systematic hydraulic sorting of carbonate and siliciclastic sediment by tidal currents.	Deposition adjacent to migrating dunes and bars and on mixed tidal flats.

Salt & microbial marsh

Channel fill & gravel bedforms on tidal flats

Siliciclastic-rich tidal flat & channels

TABLE 1 (cont.). Bouse Formation basal carbonate member facies

Facies Name	Facies #	Lithofacies description	Sedimentary structures	ichnology/ fossil content/ plant material	Bed thickness	Typical b/s ratio	Sedimentary process	Interpretation of depositional environment	
Lime mudstone with desicc-ation cracks	9	Mm-cm scale laminations and thin beds of white, gray, light pink lime mudstone. Interlaminated with mm-scale laminations of micrite or (uncommonly) pale green siliciclastic clay. Extremely rare gypsum and halite evaporites. Weathers platey. Locally high silica content. Rarely massive.	Wavy beds pinch and swell along bedding planes. Mudcracks and raindrop imprints ubiquitous on bedding surfaces	Mollusc, bivalve, Some *in-situ* clusters of barnacles. *Arenicolites, Planolites, Skolithos*	mm-cm indiv. beds	unmixed (carbonate)	Frequent exposure; green clay could record local silici. sediment influx via small catchments; Soft sediment deformation via liquefaction and fluidization induced by sediment overloading.	Lime mudstone upper tidal flats; barnacle clusters on firm or hardgrounds; rare evaporite minerals may represent deposition in a humid climate.	**Siliciclastic-rich tidal flat & channels**
Laminated rhythmic bedding	10	Planar laminated beds with rhythmic thickening and thinning. Medium- to fine-grained sand, silt, and clay alternating with lime mudstone. silt–v.f.g. sand beds. See O'Connell (2017).	Laminated; Low amplitude lenticular and wavy bedded	Incumbent anisodactyl bird tracks, <1mm-scale *Lockia, Sagittichnus,* possible *Scolicia,* possible *Selenichnites*, *Skolithos, Treptichnus*	lamina	unmixed (laminae alternate silic-carbonate)	Vertically accreted tidal rhythmites; Systematic hydraulic sorting and deposition of sediment by tidal currents; high sediment supply.	Mixed intertidal tidal flats.	
Heterolithic bedding (carb.-rich)	11	Lime mudstone, siltstones, and very fine to coarse mixed carbonate and calcareous siliciclastic sandstone. Pink, tan, white, v.f.g. to f.g. mixed-carbonate and siliciclastic sand. Small scale, weakly bimodal-bipolar, Interbedded with 3–4 cm of continuous parallel laminated fine-grained grainstone beds with fossil hash and laminated very thin beds of white lime mudstone.	Stacked wavy, lenticular, flaser bedding, ripple cross lamination with small-scale reactivation surfaces with lime mudstone drapes	Barnacle clusters <7 cm. *Conichnus, Cylindrichnus, Gastrochaenolites, Palaeophycus, Planolites, Skolithos, Teichichnus, Thalassinoides* (Fig. 16)	0.1– 10 cm (indiv. beds) 50 cm – <6 m (stacked heterolithic beds)	b/s>1 to b/s>>1	Deposition and reworking by tidal currents and declining current energy and decrease in the sand to mud ratio laterally.	Mixed intertidal flat setting & shallow subtidal bottomsets of tidal dunes and bars.	
Barnacle- & oncoid-rich grainstone	12	Well cemented barnacle and oncoid-rich coarse bioclastic grainstone, Bedding on large crossbed sets is generally tabular or sigmoidal with sharp-set boundaries. Foreset bedding can pass laterally down dip into flat lying, sandy equivalent heterolithic bottomsets, and then muddy heterolithic bottomsets. Bimodal-bipolar paleocurrents are locally present, but rare. Silici. sediment can be comprised of fine-grained sand, granules, and small pebbles. Locally, tidal-bundled crossbedded foresets alternate from bioclastic grainstone hash with <5% siliciclastic sediment, and tan-gray fine-grained sandy grainstone with ~30% siliciclastic sediment, comprising a unique form of mixed carbonate-siliciclastic inclined heterolithic strata (IHS). Can be interbedded with rare silicified, laterally extensive massive lime mudstone beds ~10 cm.	Trough crossbedding oriented obliquely to or downdip of foresets of migrating bedforms; flat-topped ripples; planar crossbedding; sigmoidal bundles, up-dip migration of ripples; IHS; rare herringbone crossbedding	Barnacle aggregate clusters <7 cm. Sparse interbedded *Thalassinoides* burrows; coralline red algae	0.1–0.5 cm (single foreset strata) 0.3- to 1.10 m (cross-set) 10 –20 cm (topset)	b/s>1 to b/s>>1	Systematic hydraulic sorting of carbonate and siliciclastic sediment by tidal currents; lateral accretion of tidal bars; dune migration; fall out of suspended fines and platy shell material during slack water stages. Lime mudstone interbeds may represent incipient flooding surfaces before full transgressive transition to FA 4.	Migrating tidal dunes and tidal bars on the lower intertidal and shallow subtidal tidal flat.	**Carbonate-rich tidal flat & shallow subtidal**
Wackestone & packstone	13	Poorly cemented wackestone and packstone barnacle oncoid hash. 5–12 cm thick beds of white, pale green, poorly sorted, unstratified to weakly stratified packstone and wackestone. Lateral equivalents of bioclastic barnacle and oncoid sandy grainstone to grainstone hash.	Unstratified	Barnacles & oncoids	5–12 cm	unmixed (carbonate)	Slightly less energy and sorting compared to F12. More fine sediment may have contributed to less cementation of this facies.		
Lime mudstone & wackestone	14	Lime mudstone and wakestone. Interbedded carbonate paper shale thin beds (3–10 cm) of very thinly laminated (1–3 mm) clay; thick massive beds of white marl with no internal structure and laminations. Locally, a cyclic lime mudstone with alternations of fissile lime mud to more resistant lime mud at intervals of ~50 cm. Silt-sized lime component is uncommon.	Lamination; Karst fissures near basin margins	Fauna is sparse in thinly laminated beds. Clams, fish fossils, snails, and ostracods Foraminifera, possible jellyfish imprints, ostracodes, *Batillaria,* possible *Paleodictyne, Planolites*	1–3 mm (individual lamina) 3–10 cm (beds)	unmixed (carbonate)	Fall-out from sediment suspended load; Karst fissures from subaerial exposure and carbonate dissolution near basin margins.	Shallow to deep subtidal; flooding of tidal facies in FA4; prior to arrival of Colorado River. Karstification is suggestive of post-depositional exposure to a humid climate. No tidal rhythmites or evidence for tides in this facies.	**shallow–deep subtidal 10–100 m**

TABLE 2. Bouse Formation basal carbonate member facies associations

Facies Association	Facies	Description	Interpretation
FA1: Siliciclastic-rich tidal flats	1, 2, 4, 5, 6, 7, 8, 9	Mixed (carbonate and siliciclastic) siliciclastic-rich interbedded sandy ripple cross-laminated strata, heterolithic bedding, and lime mudstone with desiccation cracks. Lateral facies variations common. The base is generally a matted plant-rich carbonate facies, or rarely a cobble conglomerate. Mixed siliciclastic-rich facies are interbedded with lenticular and planar crossbedded conglomerates. Extremely rare evaporites.	Siliciclastic-rich upper, mixed, and lower tidal flats flanked by salt marsh deposits. Siliciclastic sediment is likely derived from small basin-margin catchments. Association of siliciclastic sediment and carbonate sediment is likely due to carbonate super saturated waters (i.e. precipitation from seawater supersaturated with respect to carbonate) in the paleo-Gulf of California. Rare evaporites suggest a humid climate.
FA2: Tidal-channel complex	1, 3, 5, 7, 9	Concave-up strata (<15 m) with an erosional base, thinning to a few meters on the channel flanks before pinching out. Coarse conglomerate, with common scour surfaces, comprise the base of channels. Coarse conglomerate is overlain by mixed siliciclastic-rich sandy strata in channel axes. Sand-rich strata pass laterally to lime mudstone with desiccation cracks toward the outer flanks of the channel. Then, lime mudstone passes laterally to mixed silicified sandy microbial clotted carbonates with abundant vertebrate tracks at the outer-most flanks of the channel.	Deep <15 m channel systems. Orientation is uncertain because of 2D exposure. Channels filled with local catchment-derived sediment. Association of siliciclastic sediment and carbonate sediment is likely due to carbonate super-saturated waters in the paleo-Gulf of California. Unclear relationship with FA1, as FA2 erosionally cuts into FA1 as well as the underlying Pre-Bouse Miocene conglomerate. Possible deposition syn-post FA1.
FA3: Carbonate-rich tidal flats	9, 10, 11 ,12, 13, 14	Mixed (carbonate and siliciclastic) carbonate-rich heterolithic-bedded, fine-grained grainstone and lime mudstone, and well-sorted oncoid and barnacle cross-bedded, bioclastic grainstone. Extremely rare evaporites. Typical conformable vertical succession from lime mudstone with desiccation cracks into heterolithic bedded facies and then into crossbedded barnacle- and oncoid-rich bioclastic grainstone facies. Toward the basin center, crossbedded bioclastic facies pass laterally into heterolithic facies that then pass laterally into bioturbated lime mudstone.	Carbonate-rich upper, middle, lower intertidal and shallow subtidal flats. Similar environment to FA1, however, more carbonate-rich. Rare evaporites suggest a humid climate.
FA4: Shallow to deep subtidal (post-tidal)	14	Low-energy lime mudstone abruptly stratigraphically above high energy well cemented barnacle and oncoid crossbedded grainstones. Interbedded carbonate laminae, thin beds, and thick massive beds of white marl with no internal structure and laminations. Karst fissures near basin margins.	Post-tidal, shallow to deep subtidal deposition. Accumulated in roughly 10 to 100 m water depth based on sedimentology and foraminiferal assemblage (Dorsey et al., 2018). Abrupt contact from FA3 to FA4 is likely a basin-wide datum: it is a sharp traceable contact in all localities where this contact can be walked out. Fall-out from whiting events or sediment suspended load; Karst fissures from subaerial exposure and carbonate dissolution near basin margins indicates a humid climate. No tidal rhythmites or evidence for tidal processes in this facies.

heterolithic facies (F8) that pass laterally or pinch out entirely into ripple-laminated calcareous sandstone (F7) and desiccated lime mudstone (F9) (Figs. 4, 5).

The matted plant debris rich carbonate silt (F2) is generally present at the base of FA1 (Fig. 6A), sometimes associated with the F4 conglomerate facies and rare F1 cobble lag facies. These facies are overlain by interbedded ripple laminated calcareous sandstone (F7), siliciclastic-rich heterolithic bedding (F8), crossbedded gravels (F5), and lime mudstone with desiccation cracks (F9) (Fig 4, section B3; Figs. 5, 6A). Well-sorted gravels (F5) display a range of crossbedding styles from planar-tabular to distinctive convex-up geometries (Figs. 4–6A, 6B). Interbeds of carbonate-rich sand are locally present in F5 (Fig. 6A). Gravels (F5) commonly coarsen up section, have lenticular clinoform geometries, and transition down-dip into individual pebble beds and finer grained deposits (see gravel facies in Fig. 5). On gravel topsets, clotted microbial carbonate is rarely observed to encrust on pebble clasts (Fig. 6C). Well-sorted sandy calcarenite and calcarenitic sandstone (F7, Fig. 4, section B3) is common.

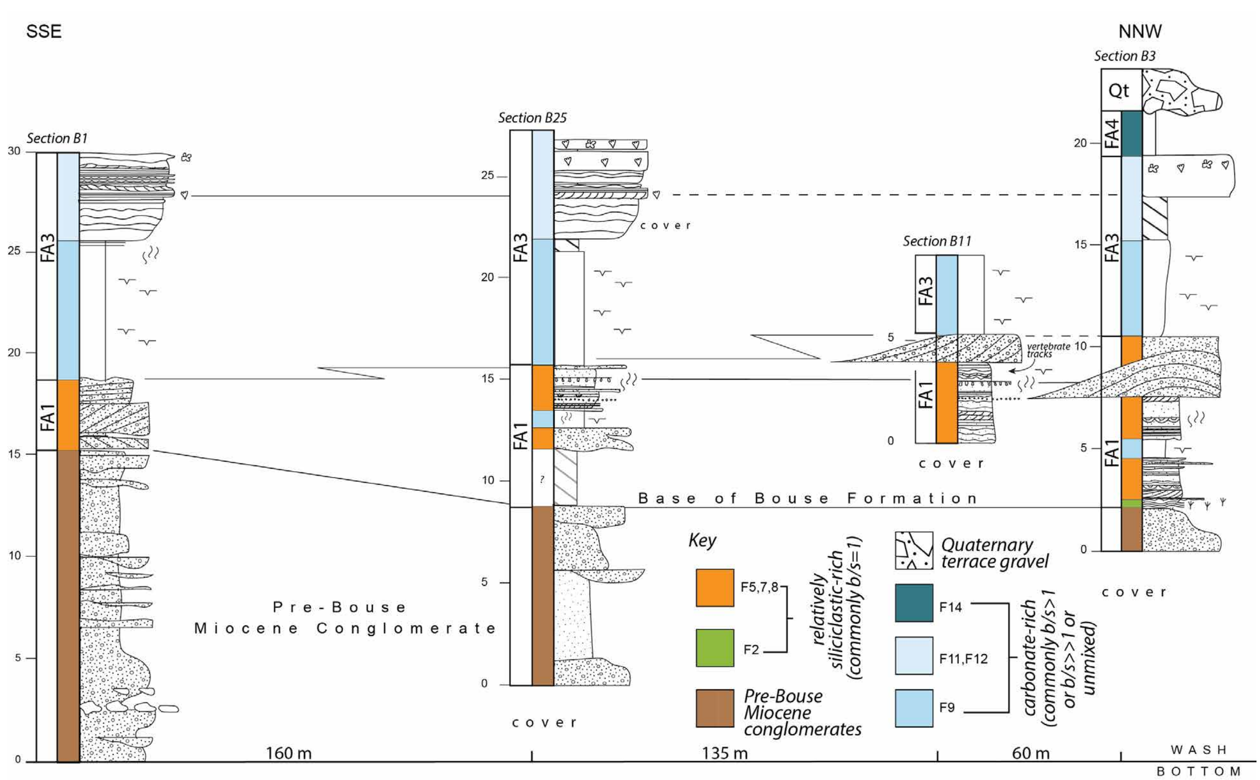

Figure 5. Stratigraphic sections and lateral relationships of FA1, FA3, FA4 from Marl Wash (see Fig. 3). Note top of sections B1, B25, and B11 are eroded.

Desiccation cracks are common on nearly every bedding plane of the lime mudstone facies (F9; (Fig. 6D); desiccation cracks are also present in matted plant debris rich carbonate silt (F2; Fig. 6E) and ripple laminated calcareous sandstone (F7; Fig. 6F). Ripple laminations with lime mudstone drapes (F7, Fig. 6G) are also common. Fossil plant debris matter (grasses, rhizoliths as root casts) (F2, Fig. 6E, 7A, B), and wavy, flaser, and lenticular bedding (F8, Fig. 7C, D) are common. Sandy calcarenite and calcarenitic sandstone is well sorted (Fig. 7E, F). There is also frequent interbedding of lime mudstone (F9), heterolithic intervals (F8), gravels (F5) and structureless calcareous sandstones (F7) (Fig 4, section B3, Fig. 6B, 8A) with parallel lamination and unidirectional ripple lamination (Figs. 4, 5, 8B). Evaporites are extremely rare, and were only observed at one locality.

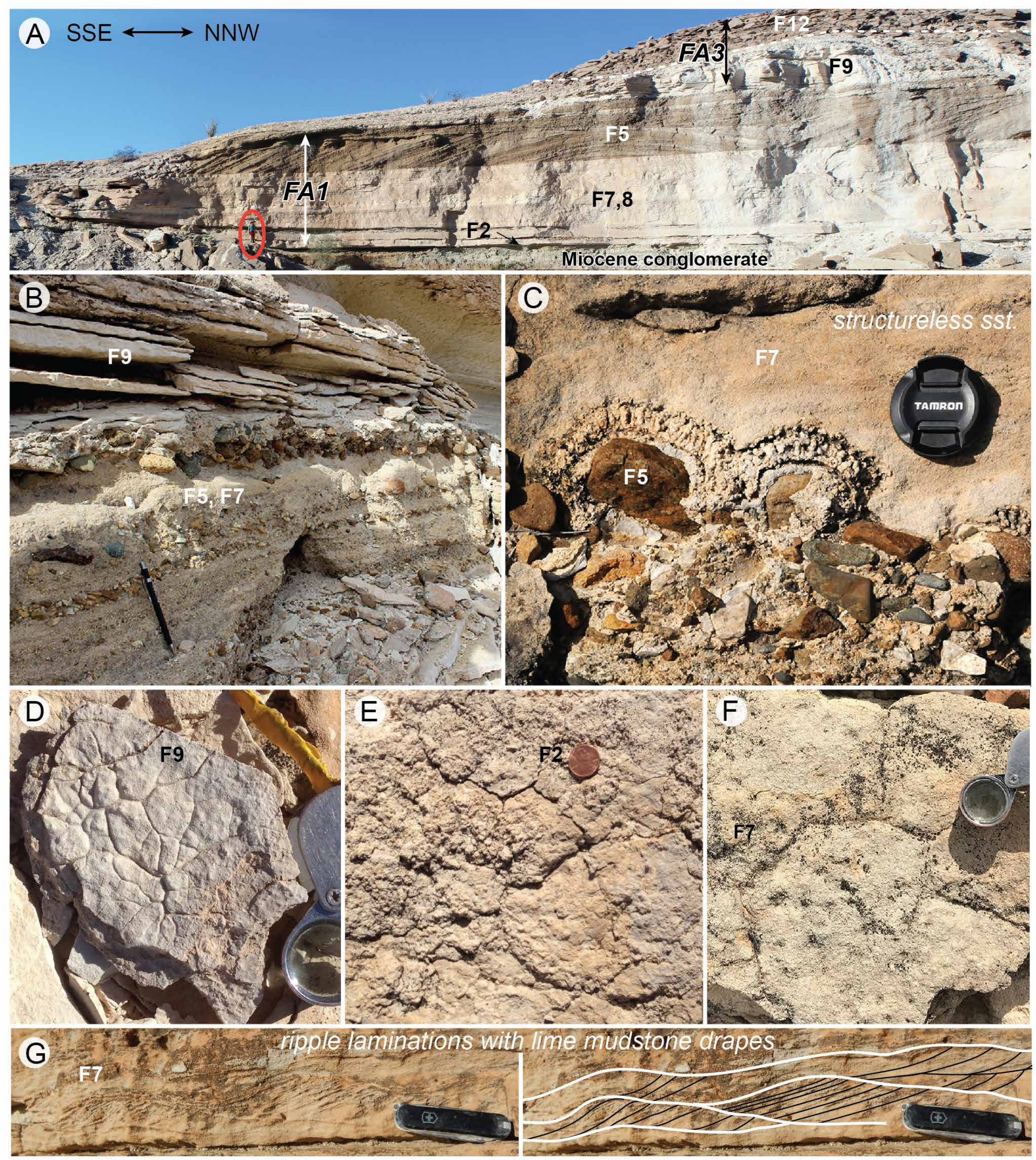

Figure 6. Facies association 1 (FA1), siliciclastic-rich tidal flats A–G: A. Overview of FA1. Note person for scale (circled) and orientation of photo. B. Interbedded gravels, sands, and lime mudstone with desiccation cracks C. rare example of clotted microbial textures on gravel clasts, lens cap 6.7 cm, sst., sandstone D. Lime mudstone with desiccation cracks. E. Bedding plane view of desiccation cracks in plant debris rich facies (F2) F. sand desiccation cracks G. Ripple cross-lamination with lime mudstone drapes, knife 5.8 cm long.

Petrography: In thin section this facies association is characterised by weakly cemented massive, mixed-composition, fine-grained calcareous sandstone with variable relative percent of carbonate and siliciclastic sediment (b/s =1, b/s<1, b/s<<1; 50–90% siliciclastic: 10%–50% carbonate; Fig. 7E, 7F). Some interbedded carbonate-rich beds, however, have less siliciclastic material ~10% (b/s >> 1) (see white carbonate-rich beds in Fig. 7D; Fig. 8A). Carbonate grains are dominated by fine-grained lime mudstone and rounded bioclasts including barnacles, gastropods, and unidentifiable fine-grained carbonate sand grains likely derived from bioclastic material (Fig. 7E–F). Grains are not compacted, and little to no clay or cement is present (Fig. 7E-F).

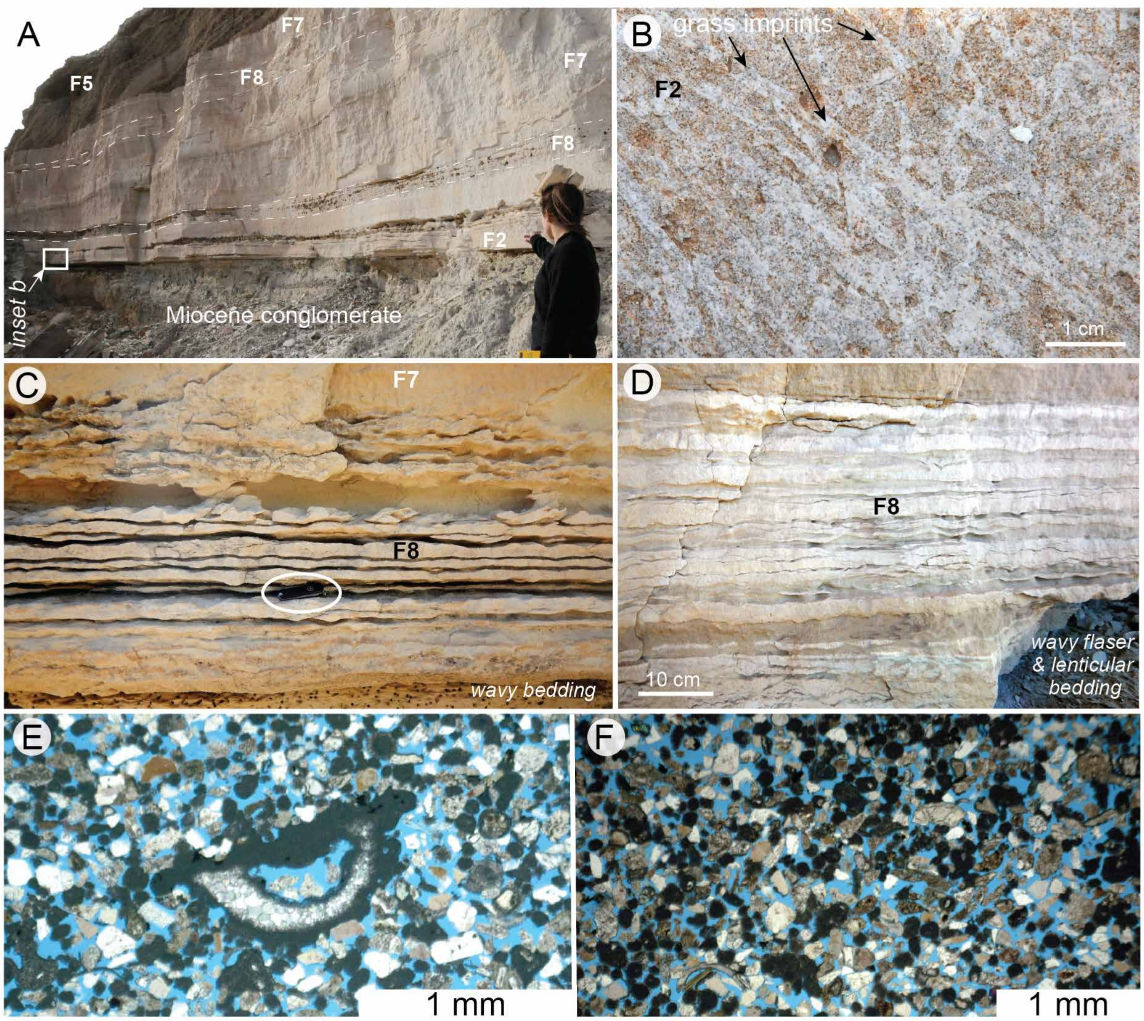

Figure 7. Facies association 1 (FA1), siliciclastic-rich tidal flats A–F. A. Undulatory plant debris rich (grasses, microbial mats, and reed casts) beds overlying Miocene conglomerate and underlying F7, F8, F5. B. Bedding plane view of matted grass(?) imprints. C. Wavy bedding, knife 5.8 cm long. D. Mixed carbonate and siliciclastic wavy, flaser, and lenticular bedding; white beds

relatively carbonate- rich b/s>>1; tan beds relatively siliciclastic-rich b/s=1 or b/s<1 E. Thin section photomicrograph shows poorly cemented calcareous sandstone with ~50:50 carbonate and siliciclastic grains. F. Thin section photomicrograph with mixed carbonate-siliciclastic grain types about ~20% carbonate grains.

Ichnology and palaeontology: Ichnofossils in FA1 include diminutive forms of *Arenicolites, Cochlichnus, Gyrolithes, Planolites,* Serpulid worm tubes, *Skolithos, Spirodesmos, Steinichnus,* possible *Selenichnites,* boxwork *Thalassinoides* (0.5–1 cm diameter), *Teichichnus, Treptichnus,* and escape burrows associated with unidirectional ripples and parallel laminations (Fig. 4, section B3; Fig. 8). In F7 and F8, *Arenicolites, Cochlichnus, Steinichnus,* boxwork *Thalassinoides* (0.5–1-cm diameter), serpulid worm tubes, possible *Selenichnites, Spirodesmos, Teichichnus,* and escape burrows associated with unidirectional ripples and parallel laminations (Table 1; Fig. 4, section B3). *Arenicolites*, *Planolites,* and *Skolithos* occur in F9 (Table 1; Fig. 4, section B3). These diminutive forms have a <10 mm penetration depth and mm-scale size, low trace-fossil diversities in bedding (1–2 forms), and sporadic low bioturbation indices (e.g., Dashtgard & La Croix, 2015; La Croix et al., 2015). Sandy facies (F7) in this association locally preserve camel (*Lamaichnium*) and horse trackways (Fig. 5, section B11).

Figure 8. Trace fossils FA1 A. *Thalassinoides* bed (arrow). Note interbedding of gravels, structureless calcareous sst., lime mudstone, few interbeds of relatively more carbonate-rich strata (white strata, b/s >>1;). Bioturbation mainly in fine-grained beds, lens cap (circled) is 6.7 cm (in all photos). Sst., sandstone; mudst., mudstone. B. Escape traces associated with unidirectional flow ripples and parallel laminations C–E. Bedding plane view of *Thalassinoides* bed with characteristic boxwork network; lens cap 6.7 cm. F. Possible Serpulid worm tubes G. cf. *Spirodesmos.* H. Possible *Gyrolithes*.

<u>*Interpretation*</u>: Plant debris rich facies (F2) was likely deposited by biological trapping of fine-grained carbonate silt and clay by reeds and grasses in a low energy, upper intertidal to

supratidal salt marsh environment. Deposition occurred during occasional flooding by baffling and sediment entrapment in highly vegetated marshes (F2; e.g., Nyman, 1993; Dashtgard & Gingras, 2005). Thin gravel interbeds (F4) may record accumulation at the base of small runoff channels or tidal creeks (Dashtgard & Gingras, 2005). Desiccation cracks (F2, F7, F9) record intermittent exposure and drying of the sediment surface between flooding and depositional episodes. Pervasive desiccation cracks (ubiquitous in F9) and rare raindrop imprints are common features of tidal flat environments (e.g., Thompson, 1975; Hardie, 1977; Shinn, 1983). Heterolithic bedding––found extensively throughout this association—is a common feature of modern tidal environments (e.g., Klein 1977; Dalrymple et al., 1991; Choi & Dalrymple, 2004; Davis, 2012). The tracks of camels and horses may have formed on sediment that was very shallow or subaerially exposed, and likely preserved via rapid burial (Davis, 2012).

Gravels (F5) were possibly tide reworked and winnowed, as suggested by their close association with tidal deposits. The convex-up form of crossbedding in well-sorted gravel (Fig. 6A) may reflect the original convex-up geometry of barchan dune bedforms, which have been documented in high-energy gravelly tidal systems (e.g., Li et al., 2014; Todd et al., 2014). Coarsening up gravels with lenticular clinoform crossbedding (F5) may represent delta mouth bars or Gilbert deltas (e.g., Postma, 1990; Kurcinka, et al., 2018) fed by small sandy and gravelly catchments along a tectonically active basin margin (Dorsey et al., 2017).

Facies Association 1 was influenced by the interaction of fluvial freshwater and marine seawater through tidal and catchment processes. This facies association is characterised by a relatively high siliciclastic component (Fig. 7, 7F) up to 8 m above the contact with the underlying Miocene conglomerate (Fig. 5). Sedimentation in FA1 was likely periodic and episodic, with heterolithic bedding typical of fluctuating tidal currents (Fig. 7C, D), bioturbated lime mudstone and heterolithic facies interbedded with gravels (Fig. 6B), and high energy calcareous sandstones that are structureless or contain parallel lamination and unidirectional cross lamination (Fig. 8 A, B). Rapid sedimentation and deposition under nonuniform decelerating flow is indicated by the presence of parallel lamination overlain by unidirectional ripples associated with escape burrows (Fig. 8B). Although there is some ambiguity in determining the amount of fluvial influence on sediments using physical sedimentary structures, episodic high energy currents may have occurred during to river floods and intercalated finer grained bioturbated units may represent deposition during interflood periods (e.g., Dalrymple et al., 2015; Kurcinka et al. 2018; Flaig et al., 2019).

Despite uncertainties, one of the best tools to understand the fluvial-marine transition is the trace fossil assemblage (e.g., Gingras & MacEachern, 2012; Hasiotis et al., 2013; Flaig et al., 2019).

The trace fossils *Gyrolithes, Selenichnites, Spirodesmos,* and boxwork networks of *Thalassinoides* are ichnogenera typical of marine environments (e.g., Häntzschel, 1975; Pemberton et al., 2001; Romano & Whyte, 2015). Ichnogenera that occur in marine, brackish, and freshwater environments include *Arenicolites*, *Cochlichnus, Conichnus*, *Lockeia*, *Planolites*, *Skolithos,* and *Treptichnus* (e.g., Jackson et al., 2016; Hammersburg et al., 2018; Flaig et al., 2019); thus, are nondiagnostic of any one palaeoenvironment. Their co-occurrence, however, with marine trace fossils suggests they represent marine organisms tolerant of freshwater influence. Low trace-fossil diversities in bedding (1–3 forms) and diminutive forms with a distinct reduction in penetration depth (<10 mm) and size (generally mm-scale), compared to normal marine forms (e.g., Gingras et al., 1999; Jackson et al., 2016), are typical of brackish-water conditions produced by freshwater and marine water body interaction in tidal settings (e.g., Pemberton et al., 1982; Dashtgard & La Croix, 2015; Jackson et al., 2016; Flaig et al., 2019).

In sum, FA1 is interpreted as recording local interbedding of salt marsh, siliciclastic rich tidal flat deposits, and nearshore gravels, consistent with tidal flats flanking a sand and gravel-rich local river catchment. Only one example of evaporite pseudomorphs (after gypsum) was observed during years of study in this facies association, indicating that evaporites are effectively absent. The paucity of evaporites, combined with abundant desiccation cracks formed by surface exposure in carbonate-rich mud flats, provides evidence for a wet humid climate during deposition (e.g., James, 1979; Rankey & Berkeley, 2012). The implied humid conditions are unlike the hyperarid modern climate of the study area, and have potential implications for understanding late Miocene to early Pliocene palaeoclimate and palaeohydrology of the lower Colorado River region.

Facies Association 2 (FA2): Tidal-channel complex

<u>Sedimentology</u>*:* This facies association (Table 2; Figs. 9, 10, 11) includes the following facies: cobble lag (F1), sandy microbial micrite (F3), crossbedded well-sorted conglomerate (F5), ripple laminated calcareous sandstone (F7), and lime mudstone with desiccation cracks (F9). This association is dominated by relatively siliciclastic-rich compositionally mixed (carbonate-siliciclastic) strata. Similar to FA1, the carbonate siliciclastic ratio is most commonly ~50% (b/s=1) (F3, F7), although there can be a high percentage of siliciclastic sediment in some beds of F7 (b/s<1). Lime mudstone with desiccation cracks (F9) in FA2 is considered unmixed carbonate

(<10% siliciclastic), and other facies of this association are unmixed siliciclastics (>90% siliciclastic) (F1, F5, rare F7).

These facies are grouped together because they are closely interbedded and laterally equivalent deposits (Figs. 9–11). Interbedded and laterally equivalent strata are encased within lenticular stratal packages that are inset into a concave up erosional base (Figs 9–11). Sandy (F7) and gravel (F5) deposits pass laterally (conformable relationship) into lime mudstone with desiccation cracks (F9) and then sandy microbial micrite (F3) with vertebrate tracks at margins of this association (Figs. 9–11). Lenticular stratal packages with an erosional base (FA2) pass laterally (erosional relationship) into FA1 in the Marl Wash location (Fig. 3). Facies association 2 is at the same stratigraphic interval as FA1 (Fig. 2), but their relationship is unclear due to the erosive contact at the base of FA2. The relationship between FA2 and FA3/FA4 is also unclear as FA 2 is erosionally overlain by Quaternary gravels (Figs. 9–11).

Interbedded gravel and sandstone that comprise FA2 are 8–15 m thick intervals that thin to <1-m thick by lateral transition to lime mudstone with desiccation cracks (F9) and sandy microbial micrite (F3) (Figs. 9, 10). The lowest deposits of a typical inset stratal package consist of thin cobble lag (F1) or thin beds of coarse conglomerate with scoured surfaces (F5) (~0.3–2-m thick) (Figs. 9 section B27; 10, 11). Gravels (F5) and sandstone (F7) commonly are overlain by lime mudstone with wavy bedding (F9) or mixed siliciclastic-rich sandy inclined to horizontal strata (F7) in the thicker parts of stratal packages (Figs. 9–11). Interbedded ripple laminated calcareous sandstone (F7) and desiccated lime mudstone (F9) are common near the margins of stratal packages, and pass laterally to sandy microbial micrite (F3) (Figs. 9–11). Some calcareous sandstone (F7) is structureless, while other interbeds of F7 display trough crossbedding, parallel laminations, and ripple laminations (Fig. 9). Intervals typically fine upward from gravels (F5) to sands (F7) (Fig. 10 A, B) and in some cases are capped by desiccated lime mudstone (F9) or sandy microbial micrite (F3) (Fig. 10 C, D; Fig. 11 A, B). At the margins of lenticular stratal packages are mixed, silicified sandy microbial micrite with irregular laminations (F3) (Fig. 9–11 C–E).

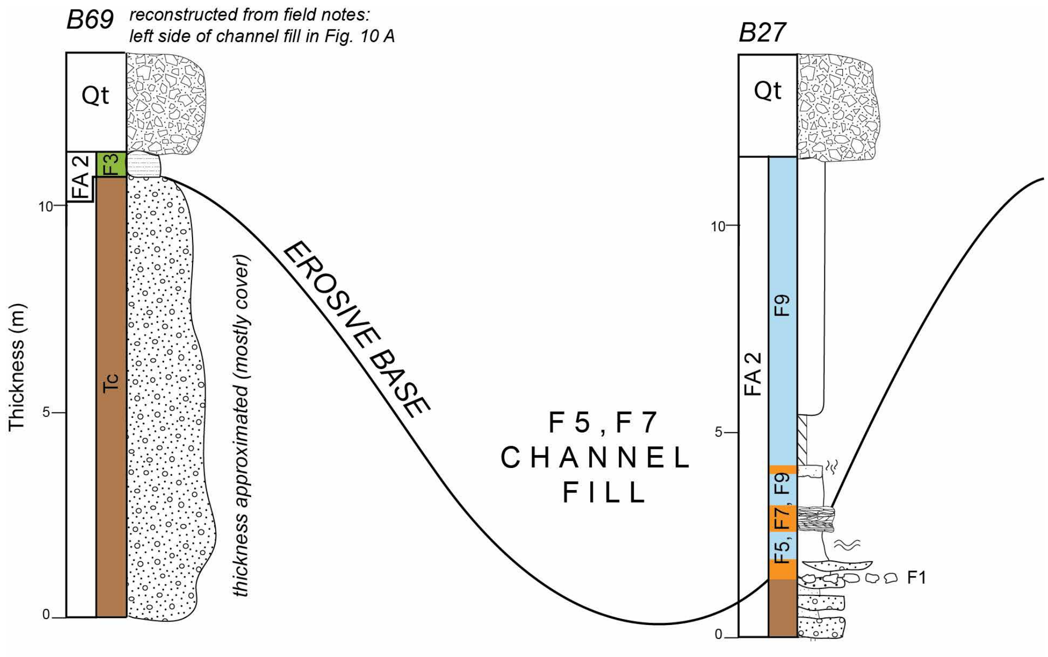

Figure 9. Facies association 2 (FA2). Section B27 was measured off mid-channel because of cliff exposure (see Fig. 10). Tc, Miocene conglomerate.

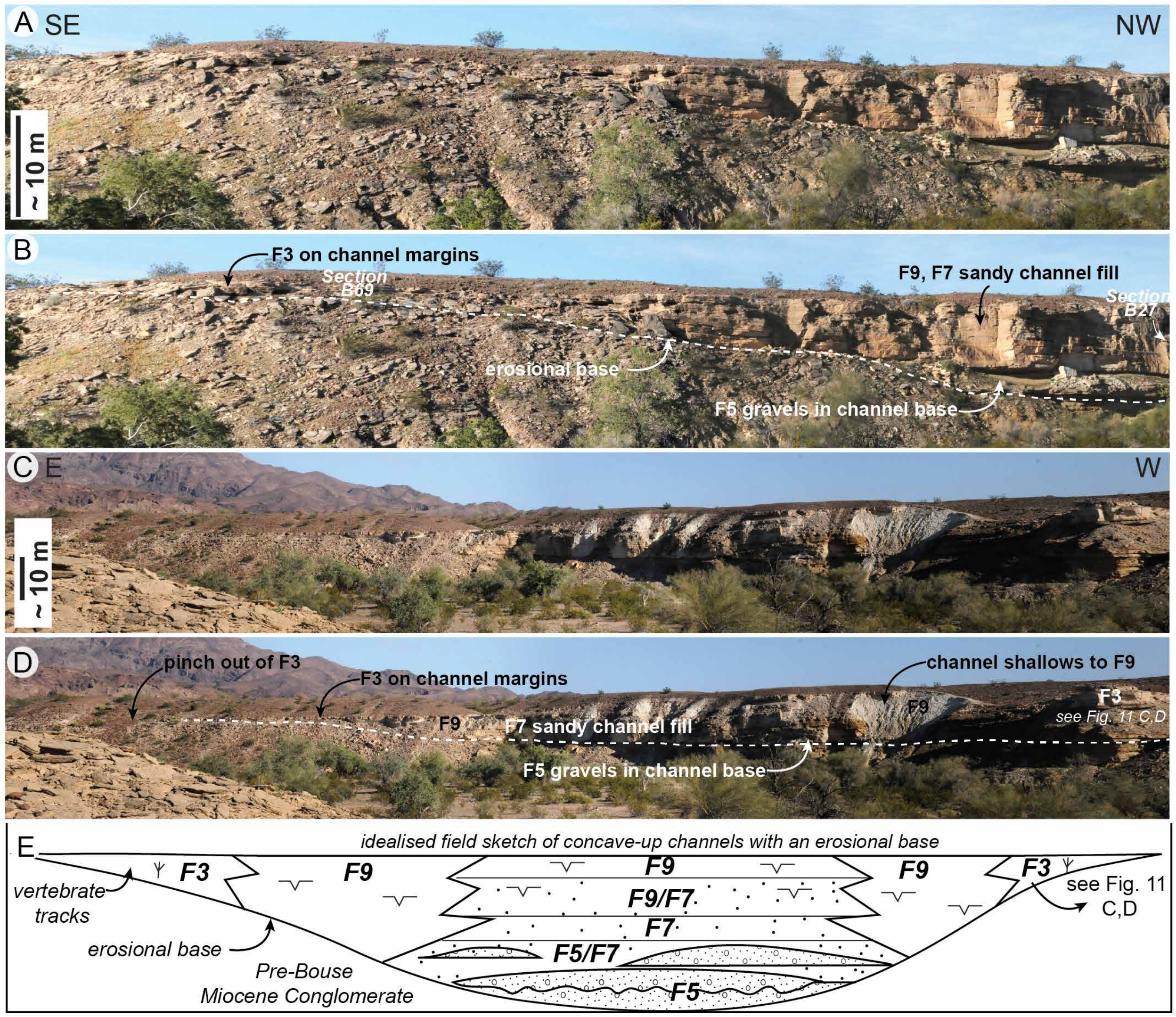

Figure 10. Facies Association 2 (FA2) channel-fill deposits. A. View looking SW at centre and edge of a typical Bouse Formation channel-fill complex. B. Annotations highlighting main features in part A; Section B27 measured out of view on right side, where outcrop was accessible. C. View looking ~south at an example of a channel-fill complex. D. Annotations highlighting main features in part C. Both examples show concave-up base of channel, concentration of siliciclastic sand in centre of channel, onlap and thinning of deposits toward channel margins, and lateral change to carbonate rich facies F9 and F3 at channel margins. E. Idealised sketch summarizing main features in A–D.

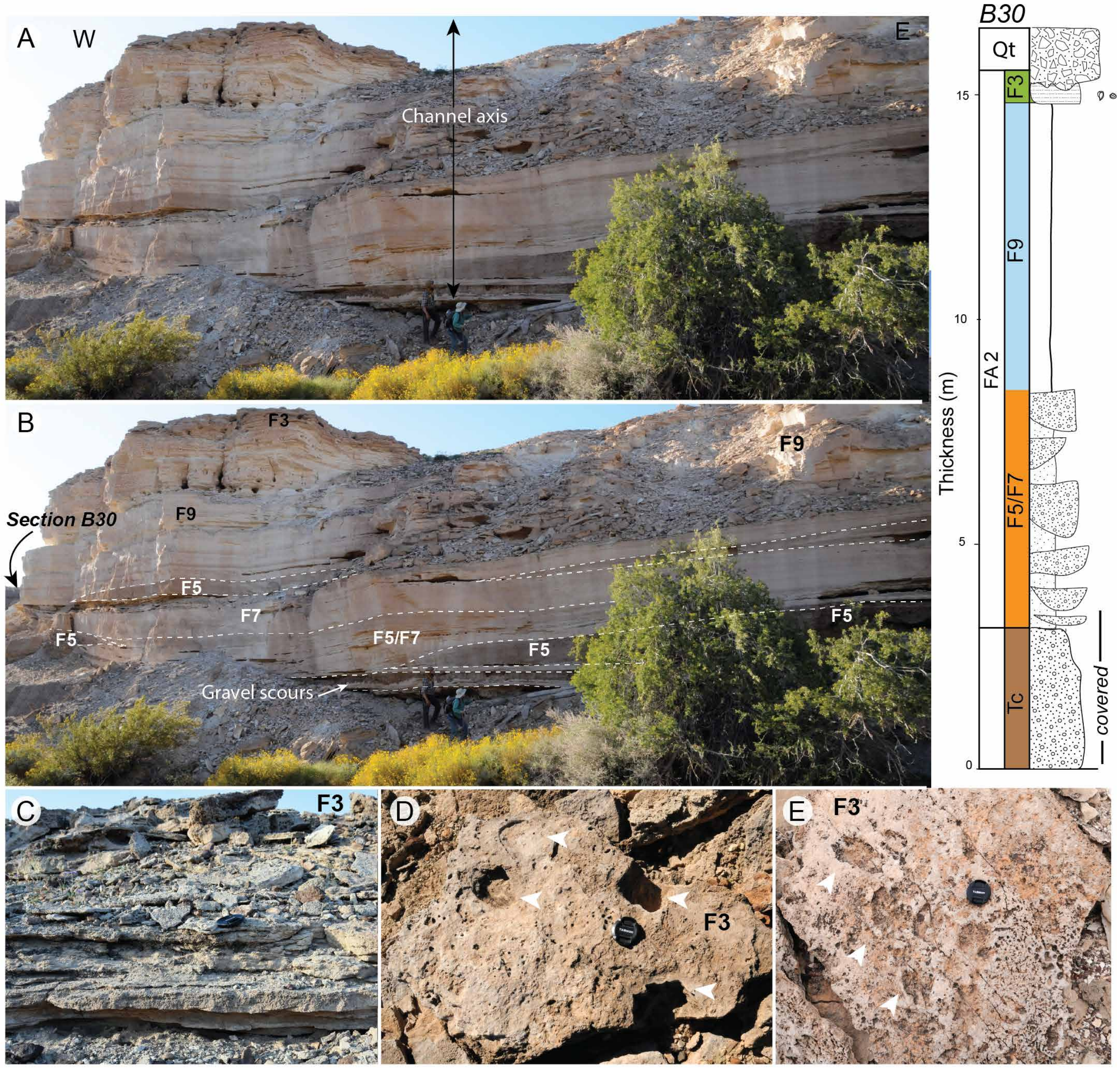

Figure 11. Facies association 2 (FA2). A. Photo looking at channel axis of this association. Note humans for scale. Orientation of photo is looking N–NW. B. Annotated photo looking at channel axis. Section B30 measured out of view on left side, where outcrop was accessible. C. Representative photo of F3, found along the channel margins. Lens cap is 6.7 cm in all photos D. Bedding plane view of horse and small elephant vertebrate tracks in F3. E. Bedding plane view of camel tracks in F3. Vertebrate tracks are common in F3.

<u>*Ichnology and palaeontology*</u>: Facies three of FA2 preserves tracks of camels, small elephants, felines, and horses (F3) (Fig. 11 C–E; Sarjeant et al., 2002; Sarjeant & Reynolds 2001). The vertebrate tracks are observed in mixed carbonate-siliciclastic silicified sandy microbial

micrite (F3) at and near the margins of concave-up lenticular stratal packages. Charophytes can be rarely present in F3 (fossil ID from Metzger, 1968; McDougall and Miranda Martínez, 2014).

<u>Interpretation</u>*:* Lenticular stratal packages with an erosional base are interpreted as channel deposits that traversed a marsh and tidal flat system. Well-cemented sandy microbial micrite with vertebrate tracks record deposition in marshes along the margins of channels. Similar to FA1, sandy microbial micrite (F3) was deposited in a low energy, upper intertidal to supratidal microbial marsh environment, as is commonly observed on humid tidal flats in the modern Bahamas (e.g., Hardie, 1977; Rankey & Berkeley, 2012). Deposition occurred during occasional flooding by baffling and sediment entrapment (e.g., Nyman, 1993; Dashtgard & Gingras, 2005). Rare charophytes in F3 may be suggestive of brackish water, possibly similar to coastal settings with charophytes in the Baltic Sea (Steinhardt et al., 2009; Bučas et al., 2019). Lime mudstone with desiccation cracks (F9) likely records upper intertidal flat deposition along channel margins adjacent to marsh systems.

Channel fill deposits comprise variable mixtures of siliciclastic sediment derived from local river catchments and carbonate sediment produced by contemporaneous calcareous organisms (microbes, barnacles, molluscs, etc.). Some siliciclastic sediment may also be reworked from underlying Miocene alluvial fan conglomerate. Well-sorted gravels were derived from small river catchments in the Trigo Mountains and reworked into migrating gravelly bedforms that filled high-energy channels. Gravels with concave up basal scour surfaces are interpreted as channel fill deposits, similar to gravel lag deposits of fluvial bars and channels (e.g., Bridge, 1993). Cobble clast horizons at the base of channel packages at some localities (FA1; Fig. 9 section B27) may represent gravel lag deposits at the channel base. Lime mudstone with desiccation cracks (F9) is interpreted to represent tidal flat environments along channel margins that pass laterally to (F3) sandy microbial micrite. Fining- and shallowing-upward transitions from gravel-sand dominated facies to fine grained lime mudstone with desiccation cracks and sandy microbial micrite (F3) with vertebrate tracks may record lateral migration, shallowing, and filling of channels.

Other than desiccation cracks and wavy bedding in F9, FA2 contains no other obvious tidal indicators (e.g., mud drapes, flaser, lenticular bedding), in contrast with FA1. Channel orientations and palaeocurrents, which could reveal the degree of tidal influence for FA2, were difficult to measure because of cliff exposures and two-dimensional (2D) representation of bedforms (Figs. 10, 11).

Facies Association 3 (FA3): Carbonate-rich tidal flats

<u>Sedimentology</u>: This facies association (Table 2; Figs. 4, 5, 12–15) includes: lime mudstone with desiccation cracks (F9), vertically laminated bedding (F10), carbonate-rich heterolithic bedding (F11), barnacle and oncoid grainstone (F12), wakestone and packstone (F13), and lime mudstone and wakestone (F14). This association is characterised by relatively carbonate-rich compositionally mixed (carbonate-siliciclastic) strata. The carbonate-siliciclastic fraction is generally ~70:30 (b/s ratio >1) (F11, F12) and, in some cases, exceeds 90% (b/s >> 1) (F9, F13, F14).

Facies of this association are grouped together because they are closely interbedded and laterally equivalent deposits (Figs. 4, 12). Centimetre- and m-scale interbedding is common in these deposits, as are lateral facies changes over the m-scale. For example, lime mudstone with desiccation cracks (F9) is commonly interbedded with carbonate-rich heterolithic bedding (F11) (rare laminated F10), and crossbedded barnacle and oncoid grainstone (F12). Crossbedded barnacle and oncoid grainstone (F12) also passes laterally into interbedded carbonate-rich heterolithic bedding (F11) and then bioturbated lime mudstone (F14) towards the basin centre (Fig. 12).

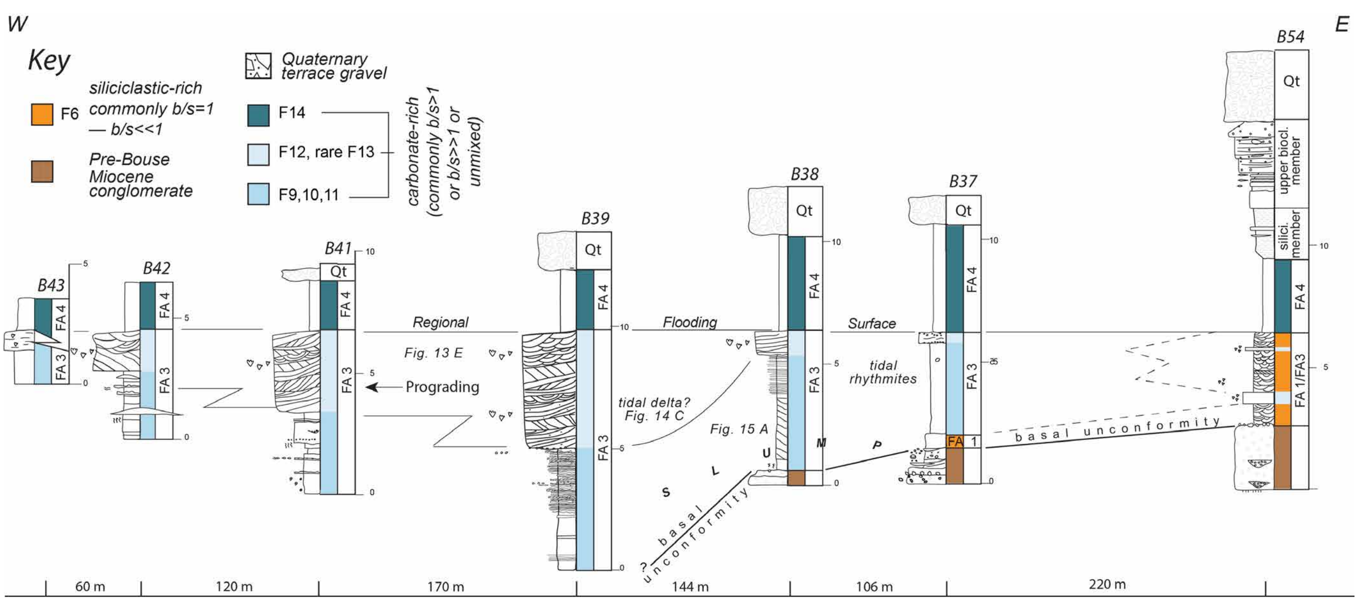

Figure 12. Stratigraphic sections and lateral relationships of minor FA1, FA3, FA4 from Big Fault Wash. See Fig. 3 for section locations.

A typical conformable vertical succession consists of an up section change from lime mudstone with desiccation cracks and rare raindrop imprints (F9) to heterolithic facies (F11, rarely F10) to crossbedded barnacle and oncoid grainstone (F12) (Figs. 4, 12, 13A). Lime mudstone with desiccation cracks (F9) consists of unmixed carbonate micrite with desiccation cracks on most bedding surfaces (Fig. 13B). Heterolithic bedded facies are mixed carbonate and siliciclastic deposits that include vertically accreted planar laminated beds with rhythmic thickening and thinning (F10) in association with incumbent anisodactyl bird tracks and lime mudstone with desiccation cracks (F9). Vertically stacked (~0.5- to 6-m thick) intervals of wavy, lenticular, and flaser bedding (F11) are also common (Fig. 12, 13C). Barnacle- and oncoid-rich bioclastic grainstone (F12) has foresets that commonly dip ~30º, and horizontal topsets display small current ripples oriented down-dip as well as obliquely to crests (Fig. 13D). Large crossbed sets are up to 3-m thick (but more commonly ~0.3- to 1.10-m thick) (Fig 12, 13E; 14A–C).

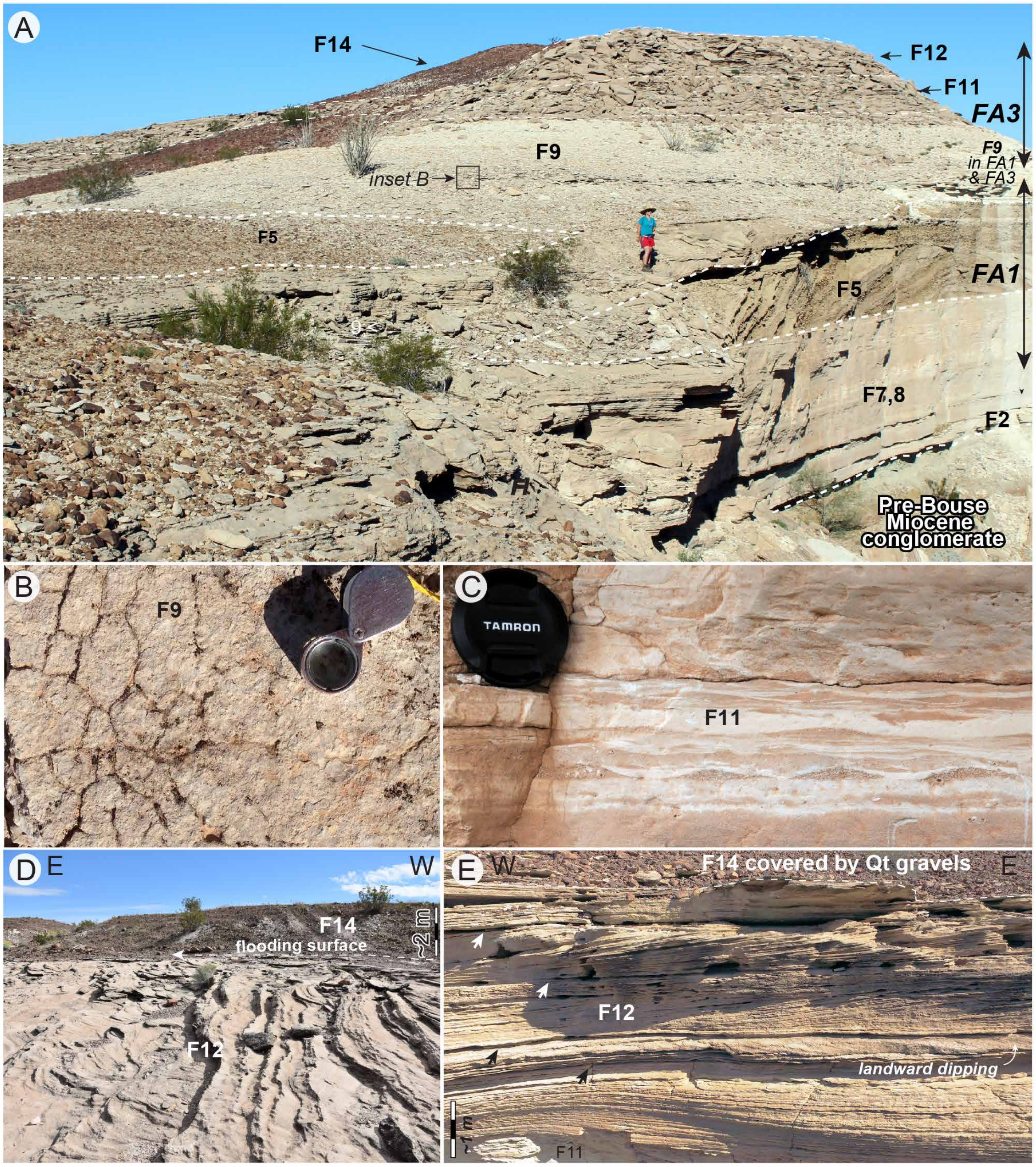

Figure 13. Facies association 3 (FA3) carbonate-rich tidal flats A–E: A. Representative example of relationship between FA1, FA3, FA4. Orientation of photos is looking NW B. Desiccation cracks on lime mudstone bedding plane surfaces C. Wavy, flaser, and lenticular bedding, lens cap is 6.7 cm D. Current ripple fans oriented obliquely to foreset bedding. Note sharp contact with FA4 (flooding surface). Orientation of photo is looking south C. Crossbedding with sharp set boundaries indicated by arrows. Orientation of photo is looking north.

Internal bedding in F12 is complex and includes bioclastic drapes on crossbed foresets (Fig, 14 B, C), well-segregated (*sensu* Chiarella & Longhitano, 2012) beds of platy-carbonate bioclastic grainstone (b/s >> 1), and fine-grained sandy grainstone (b/s > 1) (Fig. 14B). Sigmoidal bundles with rhythmic thickening and thinning of foresets are also present (Fig. 14D). Other sedimentary features include locally developed soft-sediment deformation structures (in F9 and F12; Fig. 14C; Fig. 15A) that are sometimes displaced along carbonate-siliciclastic boundaries (Chiarella et al, 2016). Flat-topped ripples (Fig. 15B) interbedded with larger scale crossbedding (0.3- to 1.10-m thick; F12) are also present. Toward the basin centre in the west, crossbedded bioclastic facies (F12) pass laterally into heterolithic bedding (F11) and bioturbated lime mudstone (F14) (Fig. 12; Fig. 15 C). Coarse-grained crossbedded grainstone (F12) thins and pinches out in both directions, toward the basin margin and the basin centre (Fig. 12).

Petrography: Thin sections reveal coarse, oncoid-bioclastic grainstone with minor to moderate subrounded to angular siliciclastic grains that are dominantly quartz, minor feldspar, and volcanic lithic fragments (Fig. 15D–F). Bioclastic grains (of variable percent and composition) include broken fragments of barnacles, gastropods, and ostracods, subspherical oncoids, and unidentifiable bioclasts (Fig. 15D–F). Bivalves in some cases are completely dissolved to create moulds (Fig. 15E). Mouldic porosity, or selective dissolution of bioclasts (Fig. 15E), is a common feature in this facies association. Cement crusts, non-isopachous fans, and variably preserved inclusion-rich, acicular carbonate cements are present (Fig. 15F). Cement fans are recrystallised but, in some cases, retain mottled sweeping extinction under crossed polars. This facies can be well cemented compared to FA1 and FA2 (compare cementation in Fig. 15F to Fig. 7E, F).

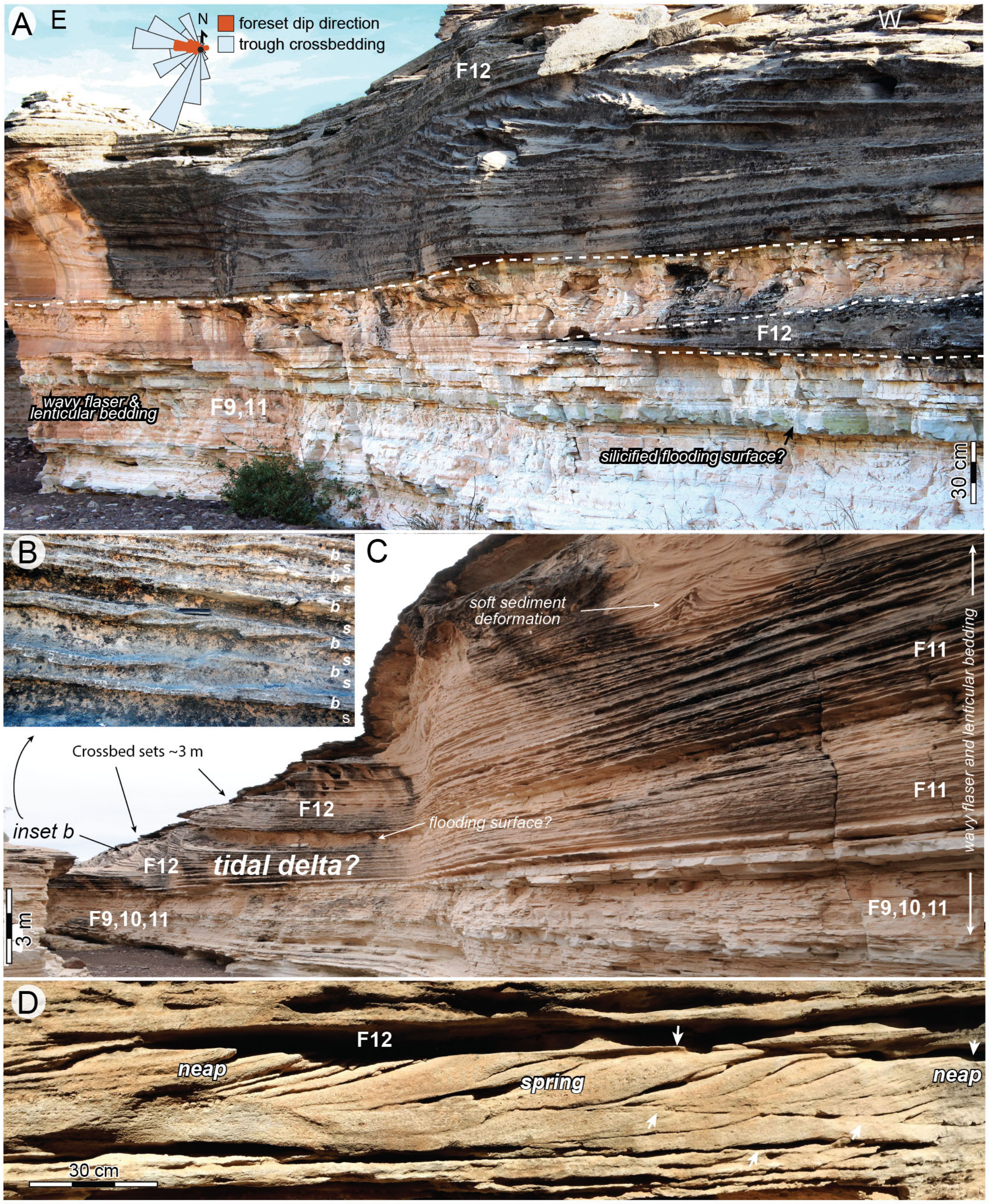

Figure 14. Facies association 3 (FA3) carbonate-rich tidal flats A–D: A. Barnacle and oncoid-rich coarse-grained bioclastic grainstone overlying heterolithic bedding and lime mudstone with desiccation cracks (F9). Orientation of photo is looking S–SE. B. Alternations of bioclastic and siliciclastic sediment in crossbed foreset, knife 5.8 cm long. C. Coarse-grained bioclastic grainstone (F12) overlying interbedded F9, 10, 11. D. Sigmoidal bundle sequence (example in O'Connell et al., 2017). Arrows denote reactivation surfaces. Thin amalgamated foresets are interpreted as neap tide bedforms, while thin and thick alternations of sigmoidal foresets are interpreted as spring tide bedforms.

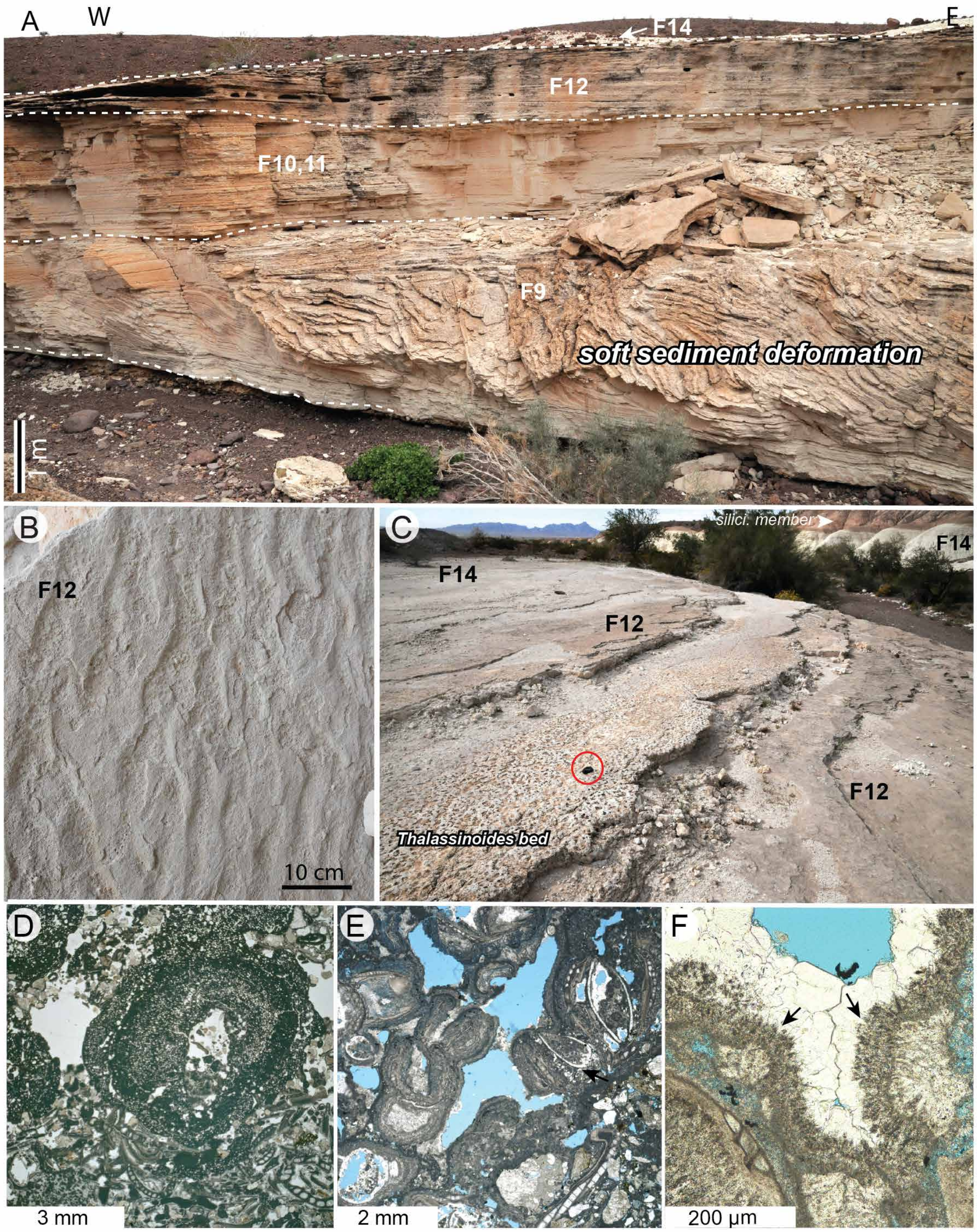

Figure 15. Facies Association 3 (FA3) bedforms and thin sections A–F. A. Soft-sediment deformation in FA3. B. Flat-topped ripples interbedded with large bedforms in F12. C. *Thalassinoides* bed in F12 passing laterally (basinward) to F14, note lens cap is 6.7 cm (circled) D. Irregular laminated oncoid grains (weakly cemented). E. Bioclasts with oncoidal irregular microbial laminations. Black arrow points to a selectively dissolved bioclast (mouldic porosity) F. Thin, inclusion-rich cement crusts and non-isopachous fans; cement generation is succeeded by clear blocky calcite cements (scalenohedral calcite). Note poor preservation of fan cement (retaining sweeping extinction) suggests a former aragonitic mineralogy preserved in calcite (black arrows).

Ichnology and palaeontology: Some beds in FA3 are bioturbated by *Batillaria* gastropods and diminutive bivalves. Trace fossils are common in heterolithic beds (mainly F11), and include diminutive forms of *Conichnus, Cylindrichnus, Gastrochaenolites, Planolites, Palaeophycus, Skolithos, Teichichnus,* and *Thalassinoides* (Fig. 4 Big Fault Wash composite section; Fig. 16A,B). These diminutive forms generally have a <10 mm penetration depth and mm-scale size (Fig. 16A,B). Trace fossils in F9 include *Arenicolites, Planolites Skolithos*; traces in F10 include incumbent anisodactyl bird tracks, < 1-mm-scale *Lockia, Sagittichnus,* and possible *Scolicia, Selenichnites, Skolithos,* and *Teichichnus.* Trace fossils in bioclastic strata (F12) are rare, but this facies can be interbedded with ~10-cm-thick, densely bioturbated beds (F14) of diminutive *Thalassinoides* (Fig. 4 Big Fault Wash composite section; Fig. 15C). Rounded aggregates of barnacle shell material up to 7-cm thick are common (Fig. 16C) *In situ* barnacle clusters are locally present on lime mudstone with desiccation-cracked surfaces (F9), particularly where deposits are interbedded and laterally adjacent to barnacle and oncoid-rich, coarse-grained bioclastic grainstone (F12) (Fig. 16D). Barnacle fragments and other grains are coated extensively by coralline red algae in this facies (Dorsey et al., 2018).

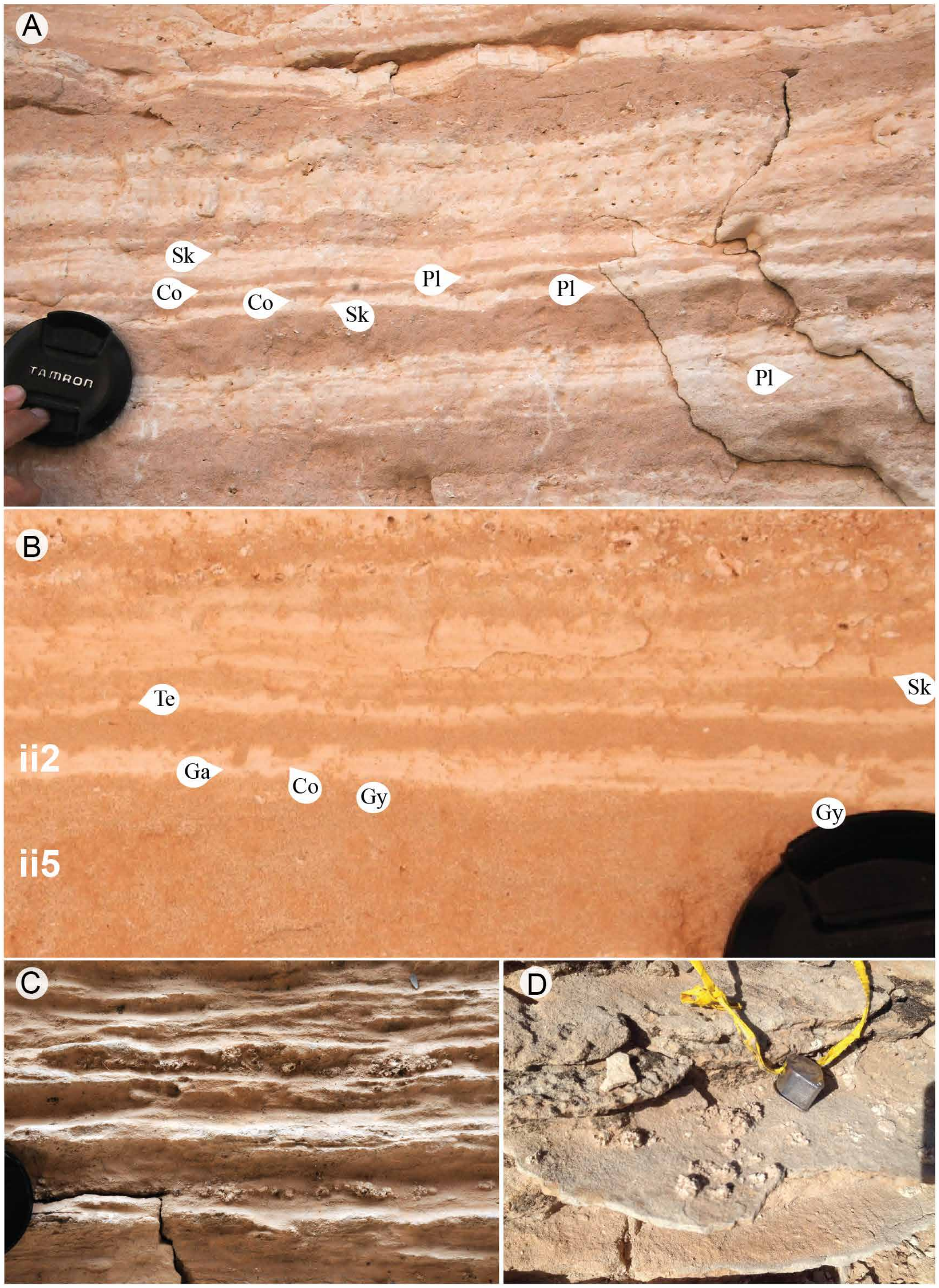

Figure. 16. Trace fossils of FA3. A, B. Diminutive traces: *Gastrochaenolites* (Ga), *Conichnus* (Co), *Skolithos* (Sk), *Teichichnus* (Te), *Gyrolithes?* (Gy), and *Planolites* (Pl). Combination of facies, trace fossils, and alternation of low-high ichnofabric indices (Droser & Bottjer, 1986) are typical of tidal & marine salinity influence, lens cap is 6.7 cm. C. Rolling barnacle aggregates, lens cap is 6.7 cm D. *In situ* barnacle clusters on firmgrounds or hardgrounds of F9.

Interpretation: Similar to FA1, pervasive desiccation cracks and raindrop imprints in fine-grained facies (F9) of FA3 record frequent exposure of mixed carbonate-siliciclastic tidal flats, a common feature of upper tidal flat environments (e.g., Klein, 1977). Heterolithic strata are interpreted to record deposition by tidal currents in intertidal to shallow subtidal environments, as evidenced by vertically stacked successions (~0.50- to ~6-m thick) of wavy, flaser, and lenticular bedding (F11). While wavy, flaser, and lenticular bedding are rarely produced by diurnal wind patterns in dryland lacustrine environments (Ainsworth et al., 2012), stacked successions strongly suggest the action of astronomical tidal processes (Davis, 2012). Vertically accreted planar laminated beds with rhythmic thickening and thinning (F10), crossbeded foresets, and sigmoidal bundles with rhythmic thickening and thinning (F12) have been interpreted as tidal rhythmites (O'Connell et al., 2017). Tidal rhythmites are especially diagnostic of a tidal influence for this association (O'Connell et al., 2017). Vertically accreted tidal rhythmites (F10) associated with lime mudstone with desiccation cracks (F9) and incumbent anisodactyl bird tracks indicate intertidal deposition in some cases. Tidal rhythmites record rapid accumulation in environments with high production of accommodation, such as in rapidly subsiding basins (e.g., Coueffe et al., 2004). Moreover, the development of cyclic rhythmites requires high sediment supply (~1 mm of sediment every ~12-hour period), which normally is only possible along channel margins or in delta-front settings (Dalrymple, 2010).

This facies association displays many diagnostic features that are widely used to identify tidal deposits, including: (1) tidal rhythmites; (2) sigmoidal bundles and bedding; (3) high degree of hydraulic sorting and segregation by grain size and composition; (4) bidirectional palaeocurrent indicators; (5) landward and seaward dipping cross strata; (6) tabular bedding with sharp set boundaries and complex internal cross strata; and (7) segregation between the siliciclastic and carbonate fraction (e.g., Boersma & Terwindt, 1981; Klein, 1970; Nio & Yang, 1991; Chiarella & Longhitano, 2012; Longhitano et al., 2012a, 2012b). Coarse-grained bioclastic grainstone in FA3 displays a high degree of sorting and segregation (including well-segregated, *sensu* Chiarella & Longhitano, 2012). Such extensive sorting and segregation by grain size and composition records extensive winnowing, reworking, and deposition by tidal currents (e.g., Chiarella & Longhitano, 2012). Soft-sediment deformation throughout this association may be an autogenic feature caused by sediment overloading in this mixed carbonate siliciclastic tidal setting (Chiarella et al., 2016). Bouse synsedimentary structural tilting (Dorsey et al., 2017) may have also induced soft-sediment deformation. Tabular bedding is typical of tidal dunes and tidal crossbedding, possibly because currents are not strong enough to produce 3D dunes, or regularly reversing currents prevent 2D bedforms from evolving to 3D bedforms (Dalrymple & Rhodes, 1995; Rubin, 2012).

This study proposes that at the majority of FA3 is intertidal based on interbedded lime mudstone with desiccation cracks (F9), heterolithic bedding (F10), and crossbedded grainstones interbedded with flat-topped ripples (F12). Intertidal barnacle- and oncoid-rich grainstone bedforms likely pass laterally (basinward) into shallow subtidal barnacle- and oncoid-rich grainstone bedforms (F12). The most basinward facies of this association is bioturbated lime mudstone and wakestone (F14). Facies 14 is interpreted to represent more distal shallow subtidal equivalents of intertidal and shallow subtidal barnacle- and oncoid-rich grainstone (F12).

Occasional bioturbated beds (F14) interbedded with (F12) may record periods of relative quiescence and colonization by marine infaunal organisms, likely during neap tides (Tape et al., 2003; Longhitano and Nemec, 2005) or incipient flooding events during marine transgression. Barnacle aggregates or balanuliths (in F11 and F12) —free-living clusters of marine barnacles that nucleate around shell fragments (Fig. 16C) —resemble mobile hardgrounds described by Cadée (2007) in the North Sea. Barnacle shell material in FA3 likely was sourced from *in situ* barnacle clusters produced on firmgrounds or hardgrounds on lime mudstone tidal flats (F9) (Fig. 16D). The presence of balanuliths is significant as these spherical aggregations are produced by continuous movement along on the sediment surface (Cadée, 2007).

The trace fossils *Cylindrichnus, Teichichnus,* and boxwork networks of *Thalassinoides* are ichnogenera typical of marine environments (e.g., Häntzschel, 1975; Bromley, 1996; Pemberton et al., 2001; Hasiotis et al., 2013; Flaig et al., 2019). Diminutive forms of *Conichnus, Cylindrichnus, Gastrochaenolites, Planolites, Palaeophycus, Skolithos, Teichichnus,* and *Thalassinoides*, with a distinct reduction in penetration depth (<10 mm) and size (generally mm-scale), compared to normal marine forms (Gingras et al. 1999), are typical of brackish-water conditions produced by freshwater and marine water body interaction in intertidal settings (e.g., Pemberton et al., 1982; Dashtgard & La Croix, 2015; Jackson et al., 2016; Flaig et al., 2019).

The poorly preserved, inclusion-rich non-isopachous crusts and fans in calcite (Fig. 15F) suggest replacement of an unstable primary mineralogy, likely aragonite or possibly high-Mg calcite marine cement (e.g., Alexandersson, 1972; Folk, 1974). Abundant, former aragonite or high-Mg calcite fibrous cements are best explained by cementation in a shallow to nearshore marine environment, where precipitation from high-Mg pore waters commonly results from fluid pumping and/or degassing (e.g., Folk, 1974; Flügel, 2004). This is consistent with other observations that support a marine environment for the Bouse Formation (O'Connell et al., 2017; Dorsey et al., 2018; Garnder & Dorsey, in press; this study). High porosity, strong fluid flow, or long exposure on the seafloor may have contributed to a higher degree of cementation in this facies association compared with FA1 and FA2.

Facies Association 4 (FA4): Subtidal Lime mudstone and wackestone

<u>*Sedimentology*</u>*:* This facies association (Table 2; Fig. 17) includes the lime mudstone and wakestone facies (F14) and is characterised by carbonate-rich strata (unmixed or b/s >>1; *sensu* Chiarella & Longhitano, 2012). This facies association only includes F14 because F14 is not interbedded with, or laterally equivalent to other facies in this FA. Facies 14 of FA4 sharply overlies mixed tidal deposits of FA3 (Fig. 12).

This association includes interbedded recessive carbonate, thin beds (3–10 cm) of very thinly laminated (1–3-mm thick) micrite, and resistant thin massive beds of white lime mudstone (F14; Table 1; Fig. 17). Carbonate deposits are typically massive (Fig. 17A, B), though near the basin centre can be locally cyclic over ~50-cm-thick bedding intervals (F14; Fig. 17C). Close to basin margins, where basin subsidence was limited (Dorsey et al., 2018), the top of FA4 includes ~0.4–1-m-deep networks of sharp margin, branching V shaped, irregular sand-filled cavities that cut the lime mudstone and wackestone host rock (F14; Fig. 17D, E). Breccia fill in such networks is composed of fine- to medium-grained grainstone, siliciclastic quartz sand, and locally derived sediment (Fig. 17D, E; Dorsey et al., 2018).

<u>*Petrography*</u>*:* Facies association 4 is composed of laminated or massive structureless lime micrite with minor clay and quartz silt (Fig. 17 F, G). Some samples show rhythmic ~1-mm-scale carbonate laminae grading up to silicified laminae (Fig. 17G).

<u>*Ichnology and palaeontology*</u>*:* Facies association 4 includes laminated lime mudstone that lacks bioturbation (Fig. 17G) and bioturbated massive lime mudstone (Fig. 17H). Bivalves, fish fossils, snails, foraminifera, and ostracods are common in bioturbated beds of FA4 (Fig. 17H; McDougall & Miranda-Martínez, 2014; Bright et al., 2016, 2018; Dorsey et al., 2018), whereas fauna are sparse in thinly laminated carbonate micrite. Trace fossils and fossils in bioturbated beds

include locally abundant bivalves and their trace fossils *Lockeia* (Fig. 17H), possible jellyfish impressions, possible *Paleodictyon,* and *Planolites* (Fig. 4, Big Fault Wash composite section).

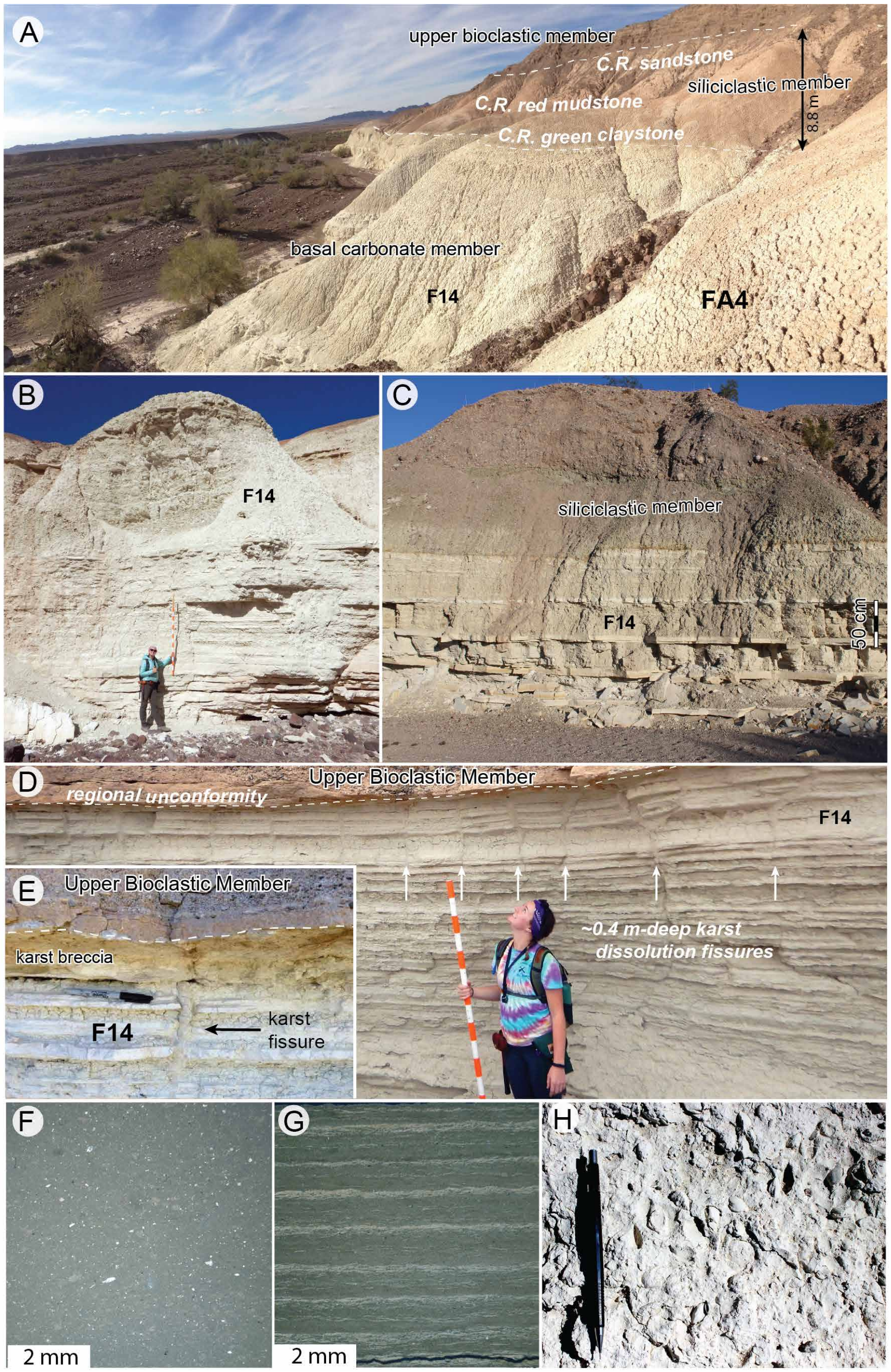

Figure 17. Facies association 4 (FA4) Lime mudstone and wackestone, A–H: A. Lime mudstone (FA4), siliciclastic member of Bouse Formation (Colorado River deltaic deposits), and upper bioclastic member (Dorsey et al., 2018). Orientation of photo is looking W–NW. B. Massive and laminated lime mudstone of FA4. C. Cyclic laminated and massive beds of lime mudstone. D–E.

Karst fissures at basin margin (Dorsey et al., 2018). F. Micrite and clay. Massive matrix with dispersed quartz silt and opaque irregular fragments, possibly organic matter. G. Laminated micrite and clay with somewhat graded microcrystalline silica replacement. White laminae are a microcrystalline silica precipitate, dark laminae are micrite and clay laminae (nontidal). H. Bedding plane view of bivalves.

Interpretation: Facies association 4 is inferred to have accumulated in 10- to 100-m water depth based the foraminiferal assemblage presented in Dorsey et al. (2018). These water depth estimates are consistent with the abundance of lime mudstone sediment in FA4 that indicates a low-energy environment protected from waves and currents (shallow to deep subtidal or lagoonal; Sanders & Höfling, 2000). Some exposures of this facies association possibly represent lagoonal environments, but its position as the most exposed distal basinward deposit and the lack of evidence for an offshore barrier system lead us to interpret most of FA4 as a low-energy shallow to deep subtidal deposit. There is no evidence for a tidal influence in FA4, as previously noted (O'Connell, 2016; Dorsey et al., 2018). Intervals of bioturbation are consistent with deposition in a subtidal environment with a relatively low sedimentation rate (e.g., Rubin & Friedman, 1977; Overstreet et al., 2003). Interbedded, thinly laminated, unbioturbated units provide evidence for occasional anoxia or suboxic conditions, or rapid deposition (such as whiting events) and burial such that beds remained undisturbed prior to burial.

Intervals of alternating resistant (laminated) and non-resistant (massive) lime mudstones (Fig. 17C) may represent climate-driven cycles or occasional development of anoxic conditions (no bioturbation). Rhythmic ~1-mm-scale laminations may represent small, cyclic changes in sedimentation or seawater chemistry. Silicification is likely a marine feature, perhaps associated with a lack of detrital input (low sedimentation) and more prolonged exposure to seawater in a low-energy environment, though a secondary diagenetic origin for the silica cannot be ruled out. Networks of ~0.4–1-m-deep, sharp margin, irregular sand-filled cavities are interpreted as basin-margin karst features. Palaeokarst features at the unconformable upper surface of FA4 record subaerial exposure and dissolution due to regional lowering of relative sea level that exposed subtidal marine strata to a humid climate before deposition of the overlying upper bioclastic member (Fig, 17D,E; e.g., Meng et al., 1997; Booler & Tucker, 2002; Dorsey et al, 2018). Karstification must have occurred post deposition of FA4, but pre deposition of the overlying Bouse upper bioclastic member (Fig. 17D, E).

Ichnology Interpretation

Trace fossils documented in this study are typical of continental, freshwater, brackish, and marine environments (Hasiotis, 2002; MacEachern et al., 2007; Gingras et al., 2012; Hasiotis et al., 2013; Figs. 8, 11, 16). Marine traces include diminutive forms of *Gyrolithes, Teichichnus,* and boxwork networks of *Thalassinoides*. Facies-crossing traces—forms that can occur in marine, brackish, or freshwater environments—include *Arenicolites*, *Cochlichnus, Conichnus*, *Lockeia*, *Planolites*, *Skolithos,* and *Treptichnus* (Fig. 8; Fig. 16). These diminutive trace-fossil forms have a distinct reduction in penetration depth (<10 mm) and size (generally mm-scale), compared to normal marine forms (e.g., Gingras & MacEachern, 2012; Jackson et al., 2016; Flaig et al., 2019). In sandy facies (F7) and in channel margin sandy microbial micrite (F3), continental trace fossils include *Celliforma*, *Steinichnus*, and vertebrate tracks and trackways produced by horses (Fig. 11D), proboscideans (i.e., elephant; Fig. 11D), and artiodactyls (i.e., camel; Fig. 11E) (Sarjeant & Reynolds 2001; Sarjeant et al., 2002; Hasiotis, 2002). Heterolithic bedded, intertidal to shallow subtidal deposits (F11) include diminutive *Conichnus, Cylindrichnus, Gastrochaenolites, Palaeophycus, Planolites, Skolithos, Teichichnus,* and *Thalassinoides* (Fig. 16A, B). Deeper water subtidal deposits include intercalated bioturbated and unbioturbated lime mudstone beds (FA4), and appear to be dominated by such horizontal forms as *Planolites, Lockeia,* and possible *Paleodictyon.* Lime mudstone upper tidal flats (F9) and intertidal and shallow subtidal tidal flats (F7–8; F12) are weakly bioturbated, bedded, and highly heterogeneous. In some cases, very low trace-fossil diversities in bedding (1–2 forms) as well as sporadic low bioturbation indices suggest deposition in the freshwater reaches or highly variable brackish portions of this mixed system, common in tidal settings with freshwater influence (e.g., Dashtgard & La Croix, 2015; La Croix et al., 2015; Flaig et al., 2019). Bioturbated beds are generally fine grained and generally do not appear to represent intervals of high sedimentation (e.g., Fig. 8A); thus, ichnofossil associations likely reflect the ambient conditions in the basin. High sedimentation rates and/or alternating high velocity currents may have also hindered bioturbation (e.g., Gingras et al., 1999; Hasiotis et al., 2013; Flaig et al., 2019).

Marine traces documented in this study are similar to marine intertidal assemblages characterised by mixed co-occurring horizontal and vertical traces including *Arenicolites, Palaeophycus, Planolites, Skolithos, Teichichnus,* and *Thalassinoides* (Gingras & MacEachern, 2012). Overall, a diminutive marine fauna and low-diversity assemblage suggest salinity stress (e.g., Pemberton, 1982; Pemberton & Wightman, 1992; Gingras et. al., 1999; Hauck et al., 2009; Jackson et al., 2016; Flaig et al., 2019). Marine infauna tolerant of brackish-water settings are generally characterised by trophic-generalist behaviours, many of which are facies crossing because of dynamic depositional conditions and variability in food resource availability and forms. They typically include *Arenicolites, Cylindrichnus, Palaeophycus, Planolites, Skolithos, Teichichnus,* and *Thalassinoides* (Pemberton & Wightman, 1992; Gingras et al., 2012), which are similar to ichnofauna documented here. The suite of brackish tolerant marine ichnofauna documented in this study is consistent with the sedimentology of the Bouse Formation, which records a setting where local fluvial catchments provided siliciclastic sediment and freshwater to the margins of a marine tidal strait.

DISCUSSION

Depositional Model

The Bouse Formation basal carbonate in the study area was deposited at the low gradient eastern margin of a marine tidal strait at the north end of the ca. 6 Ma palaeo-Gulf of California (Fig. 18A). New results from exposures south of the Palo Verde Mountains indicate that the tidal strait ran through the Highway 78 pass, connecting the palaeo Gulf of California to the Bouse inland sea (Fig. 18A; Garnder & Dorsey, in press), consistent with results of other recent studies (e.g., O'Connell et al., 2017; Dorsey et al., 2018; Garnder & Dorsey, in press). The Bouse inland sea is inferred from marine foraminiferal fauna found as far north as Parker, AZ (McDougall & Miranda-Martinez, 2014) and Bouse Formation beach and tidal flat deposits at Amboy, CA (Miller et al., 2014) (Fig. 18A). Tidal currents played a major role in the distribution and accumulation of mixed-carbonate siliciclastic facies in this system. Evidence for tidal deposition and associated subaerial exposure is indicated by pervasive desiccation cracks (mainly F9, F2, F7), flat-topped ripples (F12), rain drop impressions (F9), stacked wavy, flaser, and lenticular bedding (F8, F11), tidal rhythmites (F10, F12), sigmoidal bedding (F12), and extensive sorting and segregation by grain size and composition (F8, F7, F11, F12; e.g., Chiarella & Longhitano, 2012). On the east side of the basin (the focus of this study), palaeocurrents recorded in large crossbed forests (F12) are generally directed to the west, with a minor component to the east (Figs. 4, 13D–E, 14A, 18B). Palaeocurrents measured in trough crossbedding superimposed on larger scale crossbed foresets are more variable (F12; Fig. 13D), and probably reflect local changes in flow direction guided by the adjacent bedform crests.

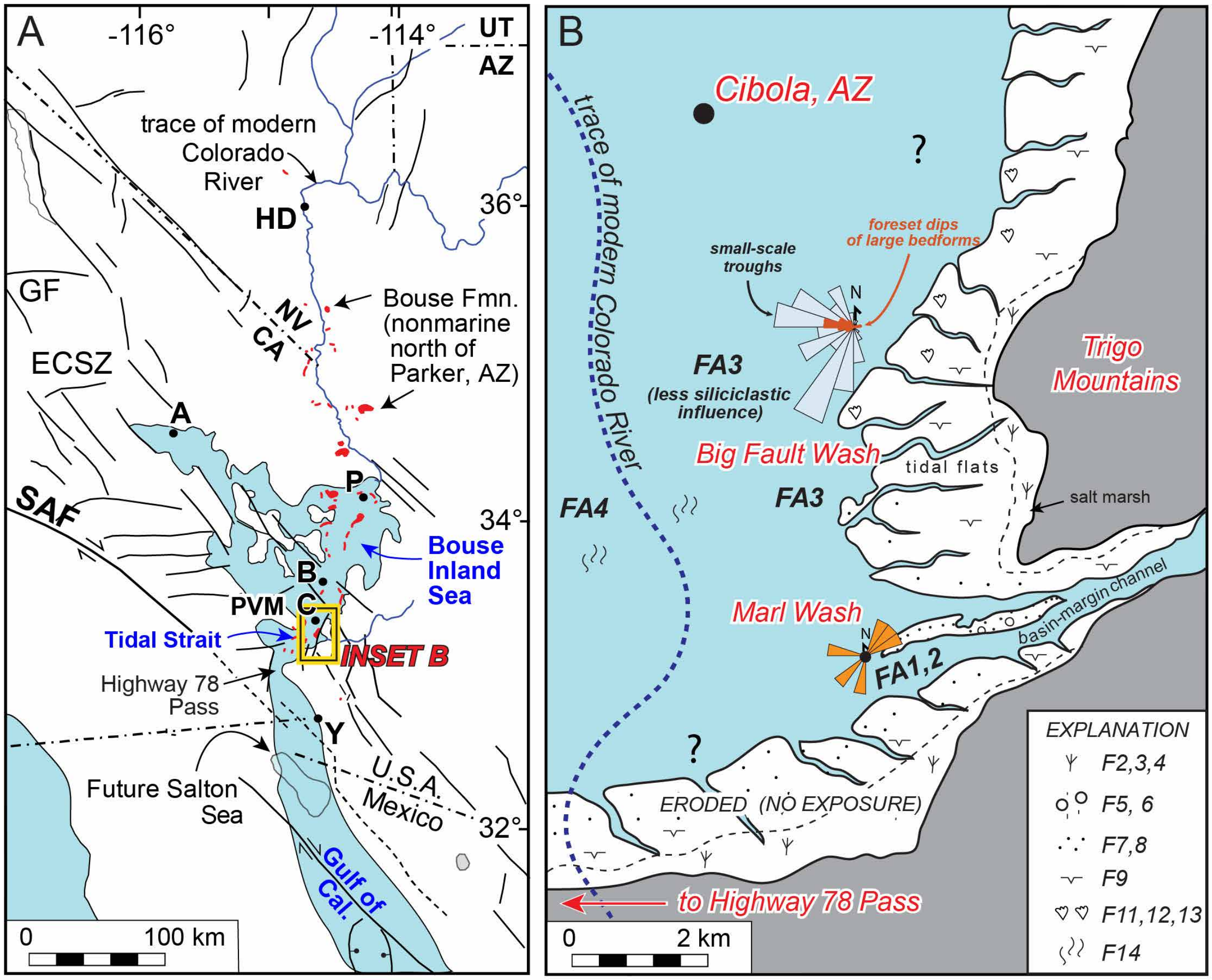

Figure 18. A. Reconstruction of the northern Gulf of California, tidal strait, and Bouse inland sea during deposition of the basal carbonate member ca. 6 Ma, prior to first arrival of the Colorado River (modified from Dorsey et al., 2018). Red patches represent modern exposures of the Bouse Formation. Note the segmented narrow connection (tidal strait; Garnder & Dorsey, in press) that connected the Gulf of California in the south to the Bouse inland sea in the north. This study documents the eastern facies at the margins of the tidal strait (inset B). B. Depositional model for the Bouse basal carbonate member southeast of Cibola, Ariz. (this study). Abbreviations: A, Amboy; B, Blythe, Calif.; C, Cibola, Ariz.; ECSZ, Eastern California Shear Zone; GF, Garlock fault; P, Parker, Ariz.; PVM, Palo Verde Mountains; SAF, San Andreas fault; Y, Yuma.

The depositional model developed for these deposits (Fig. 18B) depicts reconstructed subenvironments interpreted from detailed facies analysis. Major palaeoenvironments include siliciclastic-rich intertidal tidal flats (FA1), siliciclastic-rich channel networks (FA2), carbonate-rich intertidal and shallow subtidal flats (FA3), and shallow-deep subtidal lime mudstone (FA4). Initial deposition was dominated by siliciclastic-rich tidal flats and channel networks (FA1 and FA2) that formed above a basal unconformity produced by inundation and reworking of pre-existing alluvial fans at the eastern margin of an encroaching marine transgression (Dorsey et al., 2018). Carbonate sediment was produced *in situ* by coralline red algae, barnacles, and molluscs that were then reworked by tidal currents and hydraulically mixed with siliciclastic sand and gravel derived from local river channels in the Marl Wash area (Fig. 3, 18B). The Big Fault Wash area, which was located farther from the source of siliciclastic input, accumulated mostly carbonate-rich tidal flat deposits (FA3) with only minor siliciclastic-rich facies (FA1).

Facies relationships documented in this study show that FA3 accumulated in areas removed from siliciclastic input, whereas siliciclastic-rich FA1 and FA2 formed closer to local sources of sand and gravel (Fig. 18B). Contemporaneous deposition of FA1 and FA3 is supported by data from Big Fault Wash, where FA1 trough-crossbedded sandstone (F6) passes laterally west into carbonate-rich tidal flat deposits (Fig. 12). In Marl Wash, facies associations display an overall up-section change from FA1 siliciclastic-rich (generally b/s=1 or b/s<1) compositionally mixed carbonate-siliciclastic sediment to FA3 relatively carbonate-rich (b/s >1 and >>1) compositionally mixed deposits (Figs. 4, 5). The observed up section change from FA1 to FA3 in Marl Wash, where all facies associations are present (Figs. 4, 5), may record landward migration of distal carbonate-rich facies (FA3) over more proximal siliciclastic-rich facies (FA1). This landward shift of facies belts resulted from the same transgression that initiated tidal deposition in the study area, drowning the mouths of local rivers and trapping siliciclastic sediment progressively farther upstream in basin flanking river catchments. The lack of evaporites in FA1 and FA3, presence of diminutive, brackish-water tolerant marine trace fossils, and karstification of FA4 (post deposition of FA4 but pre deposition of the upper bioclastic member), all suggest deposition in a relatively wet and humid climate throughout Bouse Formation deposition (see section on implications for palaeoclimate).

Deposition of FA3 was terminated by increased water depths and an abrupt shift to widespread deposition of subtidal lime mudstone (FA4). The abrupt contact of FA3 with subtidal lime mudstone (FA4) (Fig. 12) is a flooding surface that represents the culmination of a long lived rise in relative sea level due to tectonically driven regional subsidence (Dorsey et al., 2018).

On the west side of the southern Blythe basin, sedimentary facies of Bouse Formation basal carbonate in the Palo Verde Mountains (Fig. 1C; Garnder & Dorsey, in press) display similarities and differences to those observed on the east side of the basin southeast of Cibola, AZ (this study; Fig 18). Similar to deposits near Cibola, facies in the Palo Verde Mountains display a transition from siliciclastic-rich to carbonate-rich bioclastic deposits that record tidally influenced sedimentation during marine transgression and deepening through time. In contrast, basal carbonate facies in the Palo Verde Mountains accumulated on a structurally active, steep basin margin on the flanks of local bedrock highs and alluvial fans, and transgressive fan fringing tidal flat deposits are overlain by crossbedded subtidal bioclastic compound dunes and carbonate sand sheets (Garnder & Dorsey, in press). The basal carbonate member of Bouse Formation in the Marl Wash area (this study) preserves a different suite of facies because it did not form near local steep topography, and instead records shallow marine inundation of a low-gradient surface. This resulted in development of a broad tidal-flat system with abundant tidal channels that traversed a much wider and shallower, lower-gradient tidal strait margin than documented in the southeastern Palo Verde Mountains. The contrasting facies associations and depositional gradients of eastern and western margins of the tidal strait reflect structurally controlled differences in palaeotopography and cross-valley basin asymmetry (Garnder & Dorsey, in press).

In sum, the margins of this tidal strait hosted a large variety of depositional processes and environments. On the west side of the basin (PVM) these environments included alluvial fans, mixed carbonate-siliciclastic fan fringing intertidal flats, and an extensive subtidal compound dune complex (Garnder & Dorsey, in press). On the east side of the basin (this study), environments included a broad belt of low-gradient salt marsh, channels, and intertidal tidal flats—both siliciclastic rich (FA1) and carbonate rich (FA3). The observed local abundance of siliciclastic sediment near the base of the basal carbonate member (FA1, FA2) and suite of brackish tolerant marine ichnofauna (FA1 and FA3), provides evidence for a local fluvial catchment that delivered siliciclastic sediment and freshwater to the east margin of the marine tidal strait, see below.

Features of the Bouse Depositional System

Siliciclastic production and evidence for freshwater-seawater mixing

Brackish water composition due to mixing of freshwater and seawater along the margins of the tidal strait is supported by evidence from sedimentology, ichnology, palaeontology, and stable isotopes, including: (1) diminutive trace fossils compared to typical marine forms (Figs. 8, 16); (2) low to very low trace-fossil diversity in bedding (1–2 forms) and sporadic low bioturbation indices (this study; e.g., La Croix et al., 2015; Dashtgard & La Croix, 2015; Jackson et al., 2016); (3) low diversity and high abundance of brackish-water tolerant diminutive marine fauna (Metzger, 1968; Smith, 1970; McDougall & Miranda-Martinez, 2014); (4) abundance of barnacles with distinctive thin plates (Zullo & Buising, 1989); (5) low oxygen isotope values in Bouse microfossils (~ -10 $\delta^{18}O$; Bright et al., 2016); and (6) positive covariation of oxygen and carbon isotopes trending to zero in Bouse Formation carbonates in the study area (Roskowski et al., 2010; Crossey et al., 2015). These data all point to significant salinity stresses due to mixing of freshwater and marine water, and require significant input of freshwater along the margins of the tidal strait.

The siliciclastic-rich composition of facies in FA1 and FA2, combined with multiple lines of evidence for salinity stress, indicate that local rivers delivered sediment and water from river catchments in the Trigo Mountains (Fig. 1C) to the margins of the tidal strait. Some siliciclastic sediment in FA1 and FA2 was likely reworked from underlying Miocene alluvial-fan conglomerate, but that cannot explain the presence of siliciclastic-rich deposits up to 8 m above the contact with the older Miocene conglomerate (Figs. 4, 5). Siliciclastic sediment in these deposits are dominated by locally abundant metamorphic and volcanic rock types, deposited before the arrival of Colorado River-derived sediment (Fig. 2; Dorsey et al., 2018). The Bouse Formation basal carbonate member in the studied area, therefore, accumulated before the arrival and integration of the Colorado River to the Gulf of California, which requires freshwater input from local rivers to produce the brackish-water composition and resulting environmental conditions documented in this study.

The abundance of carbonate in this mixed carbonate-siliciclastic marine tidal system can be reconciled with the inference of significant freshwater mixing with seawater during deposition. The underlying, bedrock-encrusting freshwater tufa that comprise the oldest unit of the basal carbonate member of the Bouse Formation accumulated in a carbonate-oversaturated system fed by deeply sourced groundwater and carbonate-oversaturated freshwater (Crossey et al., 2015). Since mixed bioclastic units of this study directly and conformably overlie the basal freshwater tufa (Fig. 2), the mixed bioclastic-siliciclastic deposits also are inferred to have formed in a carbonate-oversaturated system that favoured *in situ* deposition of organic and inorganic carbonate. Carbonate oversaturation may explain the abundance of carbonate sediment in a brackish-water system, although the controls on water chemistry of this ancient tidal system are not well understood. It is also possible that carbonate material was precipitated in shallow marine subtidal settings and transported shoreward to intertidal flats (Ginsburg, 1971).

Carbonate production

The carbonate assemblage is also an important factor in mixed carbonate-siliciclastic sedimentation. The Bouse Formation represents a mixed carbonate-siliciclastic system with a predominant heterozoan assemblage (co-occurrence of molluscs, barnacles and coralline algae; *sensu* James, 1997; James and Lukasik, 2010; Michel et al., 2018). This assemblage is similar to well documented heterozoan assemblages in modern and Pliocene Gulf of California deposits (e.g., Foster et al., 1997; Halfar et al., 2004, 2006); the lack of echinoderms and bryozoans in Bouse carbonates likely reflects brackish water conditions created by freshwater input (see above). Despite tectonically induced fluctuations in base level, siliciclastic input, and tidal versus nontidal deposition, carbonate deposition was never completely switched off during deposition of the basal carbonate member. The most siliciclastic-rich beds at the base of this unit—where fluvial input of siliciclastic sedimentation was likely strongest—contain a significant proportion of carbonate grains (commonly ~50%). A setting where siliciclastic input dilutes but never shuts down carbonate production is similar to the open coast setting described by Zeller et al. (2015), where the heterozoan assemblage continued to produce carbonate under high siliciclastic input and the proportion of grains varies as a function of siliciclastic dilution of carbonate sediment. Similar mixed carbonate-siliciclastic deposits have also been described from microtidal heterozoan skeletal carbonates in the Mediterranean (Longhitano et al., 2011; Chiarella et al., 2012).

High lateral facies variability at bedform, outcrop, and basin scales

Heterogeneity is pronounced within bedforms of the Bouse Formation in the study area. For example, foreset bedding on tidal dunes displays rhythmic alternation of siliciclastic- and carbonate-rich sediments (O'Connell et al., 2017; Fig. 14B, C). Tidal currents contributed to mixing, hydraulic sorting, and segregation of carbonate and siliciclastic grains, perhaps as a result of grain segregation over small superimposed bedforms. These results are consistent with tide induced heterogeneity of facies and bedding described in Mediterranean settings by Longhitano (2011). Outcrop and bedform scale heterogeneities observed in the basal carbonate member of the Bouse Formation are similar to bed scale compositional mixing in basin-margin facies from a variety of mixed localities reviewed in Chiarella et al. (2017). Pronounced lateral transitions in facies are also observed at the outcrop scale. For example, siliciclastic conglomerates pass laterally into fine-grained, siliciclastic-rich mixed calcareous sandstone to lime mudstone with desiccation cracks over < 200 m (FA1; Fig. 5). In FA2, sandy channel fill (F5, F7) passes laterally into channel margin sandy microbial micrite facies (F3) over 100–200 m (Fig. 9–11). In FA3, crossbedded fine-grained grainstone (F12) passes laterally into heterolithic bedding (F11) over 100–200 m (Fig. 12; Fig 14C).

In addition to variability at the bedform and outcrop scale, Bouse Formation basal carbonate displays pronounced basin scale variability. A variety of mixed carbonate-siliciclastic facies and subenvironments co-existed in the Blythe Basin (Fig. 1) with high variability of facies and carbonate percentages along strike of the palaeoshoreline. Along strike of the palaeoshoreline ~1–2-km north, facies at the base of the section are dominated by carbonate-rich tidal flat deposits (FA3) (Figs. 12, 18). Across the basin in the southeast Palo Verde Mountains (~7 km away) at the same stratigraphic interval, Bouse basal carbonate deposits include alluvial fan sheet flood and debris-flow gravels interbedded with fine-grained mixed carbonate-siliciclastic deposits of fan fringing tidal flats, overlain by high energy bioclastic subtidal compound dunes (Garnder & Dorsey, in press). The variety of facies associations from time-equivalent strata highlights variations in siliciclastic input, depositional gradient, energy, and palaeoenvironments that developed along the margins of this carbonate-siliciclastic tidal strait (Fig. 18).

Spatial patterns summarized here are similar to carbonate-rich tidal flats adjacent to siliciclastic-rich tidal flats documented in Spain by Bádenas et al. (2018). Schwartz et al. (2018) also found a wide array of contemporaneous mixed carbonate-siliciclastic environments in the Neuquén Basin of Argentina, and postulated that the variety and complexity of mixed carbonate-siliciclastic settings are related to both the proportion of carbonate and siliciclastic production, and such dominant marine transport processes as storm, shelf, and tidal currents. Similar local variability has also been documented from the Pleistocene Apennines (Italy), where four coastal wedges show variable stacking patterns and variable mixed carbonate-siliciclastic ratios just ~2-km apart from each other, interpreted to result from variable sediment supply and local syndepositional tectonics that controlled differential subsidence and uplift (Chiarella et al., 2019). Synsedimentary structural tilting controlled the stratigraphic architecture of the Bouse Formation (Dorsey et al., 2017) and may have also exerted an influence on the distribution of siliciclastic-rich versus carbonate-rich facies (Chiarella et al., 2019).

Sedimentary Hydrodynamics

During intervals of tidal deposition (FA1–FA3), strong currents in this tidal system contributed to mixing of carbonate and siliciclastic sediment. Data suggest that mixing of carbonate-siliciclastic grains was best developed during transgression due to rising relative sea level (see Dorsey et al., 2018, for sequence stratigraphic interpretation). Zeller et al. (2015) proposed a similar process in which the transport of siliciclastics was strongest during transgressive phases, allowing for enhanced transport of siliciclastic grains via an along-shelf current system that was most active during times of rising relative sea level in the Neuquén Basin of Argentina. Results from the basal member of the Bouse Formation in the southern exposures along the Colorado River (this study) suggest that sustained transport and reworking by tidal currents was the main process responsible for thorough mixing of carbonate and siliciclastic grains. The model of tidal mixing—along the margins of a geographically restricted tidal strait (Fig. 18) —is similar to the tidal mixing model of Bádenas et al. (2018) in the Mesozoic Galve Sub-basin, Spain, though the sediments deposited in the open coast tidal setting of that study were more influenced by storms and waves than the sediments of the Bouse Formation.

Evolution of the Bouse system

Implications for basin evolution

The abrupt transition to lime mudstone and wackestone (FA4), which lacks tidal features, represents widespread deepening associated with a relative sea level rise (this study; O'Connell et al., 2016). Intertidal conditions possibly continued around the retreating margins of the basin as the basin deepened (e.g., Longhitano et al., 2014). Alternatively, it is possible that hydrodynamics changed due to a rise in relative sea level and the basin fell out of tidal resonance as it passed out of the tidal-amplification window (e.g., Pugh, 1987; Sztano & De Boer, 1995). Recent studies show that this regional marine transgression took place during a period of negligible to slow eustatic sea level fall, which requires subsidence in a tectonic lowland at the north end of the Gulf of California to produce deepening of marine waters through time (Dorsey et al., 2018; Umhoefer et al., 2018). The tidal deposits of the Bouse Formation are now exposed at 100–300 m above sea level, requiring post-Miocene uplift of this basin to modern elevations in the lower Colorado River corridor (O'Connell et al., 2017; Garnder & Dorsey, in press).

The Bouse Formation basal carbonate member in the study area records local episodes of shallowing due to aggradation and progradation of tidal deposits against the backdrop of regional marine transgression. For example, gravel and sandy beds in tidal channel systems (FA2) display shallowing upwards into desiccated lime mudstone (Fig. 10C, D, 11A, B), and siliciclastic-rich tidal flats shallow up section from sandy lower and mixed tidal flats to upper tidal flat desiccated lime mudstone (Figs. 4, 5). Tidal bedforms also overlie possible incipient flooding surfaces (Fig. 14A, C) stratigraphically beneath the abrupt and widespread transition to shallow to deep lime mudstones (Fig. 4; FA4). Observed shallowing-up intervals represent exceptions to an overall basin wide regional deepening up progression from intertidal (FA1) to intertidal and shallow subtidal (FA3) to subtidal (FA4) sedimentary deposits (Homan, 2014; Dorsey et al., 2018). Deepening of tide-influenced deposits, as recorded in the abrupt transition to subtidal facies association FA4, occurred when vertical aggradation of tidal sediments was outpaced by subsidence and associated rise in relative sea level. Above the FA3-FA4 contact, input of siliciclastic sediment from nearby river catchments was nearly completely shut off and effectively removed as a component of this depositional system (FA4), highlighting the important control of relative sea level on mixed carbonate-siliciclastic sedimentation (cf. Van Siclen, 1958; Wilson, 1967).

Implications for late Miocene–early Pliocene palaeoclimate

Deposits of wide channel belts (FA2) with sandy microbial micrite supratidal facies (F3) in the Bouse Formation strongly resemble non-evaporative deposits typical of modern humid tidal flats in Andros Island, Bahamas (e.g., Rankey & Berkeley, 2012). Indeed, the concentration of salt marsh deposits (with possible microbial mats) in these settings (F1–3 in FA1 and FA2), the lack of evaporites, and common occurrence of channel deposits (FA2) are characteristic of the *'humid channelled belt'* tidal flat morphotype defined in these settings (e.g. James, 1979; Shinn, 1983; Wright, 1984). In contrast to humid tidal flat deposits represented by FA1 and FA2 of this study, the present-day northern Gulf of California is a hyperarid sabkha tidal flat system with rainfall of only 50–100 mm/year (Thompson, 1975; Ezcurra & Rodriguez, 1986). The modern northern Gulf of California is an evaporative macrotidal basin where evaporation rates of ~2.0–2.5 m/year produce enhanced salinities of 35–37 per mil in coastal areas (Bray, 1988; Lavín et al., 1998; Lavín & Marinone, 2003; Norris, 2010). In this setting, supratidal and intertidal flats are characterised by extensive halite and gypsum precipitation in distinct layers and as intrasediment crystals (Thompson, 1975; Castens-Seidell, 1984; Castens-Seidell & Hardie, 1984). Thompson (1975) described much of the modern northern Gulf sediment as 'barren mudflats and salt flats' where gypsum and halite make up significant constituents of the mud. Mud laminae are commonly deformed and ruptured due to extensive evaporitic crystallization, forming chaotic clay-evaporite mixtures (Thompson, 1975). Salt marshes in the northern Gulf of California are characterised as sabkha arid marshes (e.g., Morzaria-Luna et al., 2014; Kearney & Fagherazzi, 2016), with both unvegetated and mixed (vegetated and non-vegetated) banks, abundant evaporites, and weak soils produced by dissolution and recrystallization of salts (Thompson et al., 1975; Glenn et al., 2006).

While tidal cyclicity in the late Miocene to early Pliocene Bouse marine setting may have been similar to that of the modern Gulf of California (O'Connell et al., 2017), considerable differences exist between modern and ancient styles of sedimentation. Sediment in the modern Gulf of California tidal flats is mainly sourced from the Colorado River and reworked by tides (Thompson, 1975), whereas sediments of the basal carbonate member of the Bouse Formation accumulated before arrival of Colorado River sediment. The Bouse Formation basal carbonate in the study area lacks evaporites and contains no indicators of evaporite dissolution (i.e., solution collapse breccias), whereas the modern Gulf of California is characterised by an abundance of evaporites with deformed and ruptured beds (Thompson, 1975; Castens-Seidell, 1984; Castens-Seidell & Hardie, 1984; Glenn et al., 2006). Similar differences are observed between modern tidal systems in contrasting climate regimes, such as the well-studied arid sabkha flats in the Persian Gulf versus humid tidal flat and channel systems in the Bahamas. The arid Persian Gulf, with <100 mm/yr rainfall, hosts abundant gypsum and anhydrite evaporites (Purser, 1973; Lokier et al., 2013), while in the humid Bahamas (>1200 mm/yr rainfall), evaporites are ephemeral or absent (Shinn & Ginsburg, 1964; James, 1979; Shinn, 1983; Wright, 1984; Rankey & Berkeley, 2012).

Multiple lines of evidence summarized earlier indicate that conditions during deposition of the upper Miocene to lower Pliocene Bouse Formation in the study area were considerably wetter than the present day arid climate of the southwestern U.S. and northwest Mexico. This finding is consistent with studies that document a humid climate with widespread lakes in the western and southwestern U.S. during Pliocene time (Thompson, 1991; Forrester, 1991; Thompson & Fleming, 1996; Remeika et al., 1998). Comparison of modern El Niño events to late Miocene–early Pliocene palaeoclimates (Molnar & Crane, 2007), global compilations of palaeovegetation and climate patterns (Salzmann et al., 2011; Winnick et al 2013), and hydrologic modelling of palaeolakes (Ibarra et al., 2018) all indicate that the late Miocene to early Pliocene climate in the southwestern USA was significantly wetter than today. In the Lake Mead region east of Las Vegas, Nevada, USA, increasing freshwater inflow to a network of late Miocene playa lakes caused the lakes to become progressively larger, fresher, and more interconnected, resulting in a change through time from evaporite accumulation in small depocenters to widespread deposition of freshwater lacustrine carbonates by ca 5.6 Ma (Crossey et al., 2015; Faulds et al., 2016).

Chapin (2008) suggested that tectonic opening of the Gulf of California caused increased advection of water vapor to the southwestern U.S. and intensification of the North American monsoon by ~6 Ma, resulting in increased precipitation and lake overflows that drove downward integration of the Colorado River. The late Miocene transition from smaller evaporite basins to larger lakes with freshwater limestones in the Lake Mead region (Faulds et al., 2016) is consistent with this idea, though the ubiquitous occurrence of Pliocene wet conditions throughout the western U.S. (Winnick et al., 2013) suggests that Pliocene moisture was not sourced solely from southerly monsoonal flow. Low stable isotopes that display linear covariation along a trend to seawater values (Roskowski et al., 2010; Crossey et al., 2015) in tidally influenced carbonates that predate arrival of the Colorado River (Dorsey et al., 2018; this study) point to input of freshwater from local rivers that may have been fed by strong monsoonal precipitation, though the relative contribution of monsoonal vs. continentally derived river waters is unknown.

Implications for mixed carbonate-siliciclastic tidal deposits

Improved models for ancient mixed carbonate-siliciclastic sedimentation require an understanding of the processes that control carbonate deposition, siliciclastic input, and mixing of grain types. These processes extend beyond the singular control of base level, and include other important factors such as carbonate assemblage, climate, tectonic setting, and modes of sediment transport (e.g., Tcherepanov et al., 2008; Zeller et al., 2015; Chiarella et al., 2019). The Bouse

Formation is a well-exposed example of an ancient mixed carbonate-siliciclastic tidal setting where the carbonate assemblage, basin geometry, tidal cyclicity, and tectonic setting are relatively well constrained by prior studies and modern processes in the nearby Gulf of California. For example, the basal carbonate member of the Bouse Formation may have had a tidal cyclicity similar to the modern northern Gulf of California (O'Connell et al., 2017). In the Bouse setting, fault-controlled tectonic subsidence produced a rise in relative sea level at the northern most end of the palaeo-Gulf of California (Dorsey et al., 2018). Syndepositional faulting and structural tilting during deposition of the Bouse Formation (Dorsey et al., 2017) may have also influenced the mixed carbonate-siliciclastic composition and stacking of sedimentary packages over short distances between Marl Wash and Big Fault Wash (Figs. 3, 18; similar to Chiarella et al., 2019). These deposits likely accumulated in a wet and humid climate, in contrast to the hyperarid climate of the modern Gulf of California. High rates of siliciclastic input to the carbonate-producing basin were likely influenced by the tectonically active setting and high annual precipitation.

The Bouse Formation has heterogeneity at the bedform, outcrop, and basin scale. Understanding bed- and outcrop-scale heterogeneities is important for hydrocarbon exploration because mixed facies are common and are characterised by strong contrasts in permeability and porosity that may influence flow migration and reservoir evolution (e.g., McNeill et al., 2004; Ainsworth, 2010; Chiarella et al., 2017). For example, studies of the Delaware Basin (USA) show that a significant portion of hydrocarbon production comes from mixed carbonate-siliciclastic seafloor fans that differ significantly from their pure siliciclastic equivalents (Kvale et al., 2019). The high lateral facies variability documented in this study at the basin, outcrop, and bedform scale indicate that future study of this and similar mixed carbonate-siliciclastic settings is needed for improved facies models and understanding of mixed tidal hydrocarbon reservoirs.

CONCLUSIONS

Integrated sedimentologic, stratigraphic, petrographic, and ichnologic data from the basal carbonate member of the Bouse Formation in the southern Blythe basin provide a record of deposition at the margin of a marine tidal strait near the north end of the late Miocene to Pliocene Gulf of California. These deposits comprise 14 facies and four facies associations that accumulated before arrival of siliciclastic sediment from the Colorado River. Trace fossils are indicative of terrestrial, freshwater, brackish, and marine palaeoenvironments, consistent with sedimentological interpretations. The main conclusions and implications of this study are summarized below:

1. This study documents depositional processes and sedimentary environments at the margin of a transgressive tidal strait near the north end of the ~6-Ma Gulf of California.
2. This study proposes that relatively siliciclastic-rich heterolithic sediment, siliciclastic gravels and sands, and lime mudstone with desiccation cracks accumulated in tidal flat deposits with a fluvial influence (FA1). Lenticular stratal packages with concave up erosional bases (FA2) are interpreted as tidal-channel deposits. Relatively carbonate-rich heterolithic sediment, lime mudstone with desiccation cracks, and crossbedded bioclastic grainstone (FA3) accumulated in carbonate-rich intertidal to shallow subtidal environments. Finally, lime mudstone (FA4) accumulated in low energy shallow to deep subtidal settings.
3. An abrupt stratigraphic transition from tidal deposits (FA3) to low energy subtidal lime mudstone (FA4) represents a widespread flooding surface associated with a regional rise in relative sea level. Relative sea level rise resulted from tectonically controlled subsidence in the late Miocene to early Pliocene northern Gulf of California.
4. Evidence from palaeontology, ichnology, and sedimentology provides a clear record of freshwater input and brackish water conditions due to freshwater-seawater mixing in a humid climate with high annual precipitation. This finding requires that the climate during deposition was significantly wetter than the present day arid climate of the study area, consistent with other studies that document a humid climate with widespread freshwater lakes in the western and southwestern U.S. during late Miocene to early Pliocene time.
5. Mixing of carbonate and siliciclastic sediment was most common during transgression. The relative percentages of carbonate-siliciclastic grains is a function of siliciclastic input from catchment sources, *in situ* carbonate production, tidal mixing, and relative sea level.
6. Facies variability is pronounced at bedform, outcrop, and basin scales: individual foresets are segregated into their carbonate-siliciclastic fractions, siliciclastic-rich strata pass laterally into carbonate-rich strata over <200m along strike, and siliciclastic-rich tidal flats (FA1) are present at the same stratigraphic level as carbonate-rich tidal flats (FA3) over just ~2km along strike of the palaeo shoreline. Low-gradient facies associations (this study) are present at the same stratigraphic level as facies recording transgression of a steep rocky shoreline on the opposite side of the basin. The observed facies variability along the margins of a tidal strait highlights the importance of characterising mixed carbonate-

siliciclastic processes and environments for an improved understanding of mixed-composition outcrops.

ACKNOWLEDGMENTS

We appreciate constructive reviews by Robert Dalrymple, Domenico Chiarella, Beatriz Bádenas and one anonymous reviewer. We also appreciate comments from Chief Editor Giovanna Della Porta and the Associate Editor John Reijmer. This study benefitted from discussion with Kevin Gardner, Malcolm Wallace, Murray Gingras, William Kearney, Kyle House, Brian Gootee, Jordan Bright, and many others. BOC thanks Logan Wetherell, Avery Maverick, Jordan Lanni, and Kristin Franks for field assistance. Funding was provided by the Society for Sedimentary Geology, International Association of Sedimentologists, Geological Society of America, and the National Science Foundation (grant EAR-1546006 to Dorsey). Ashleigh Hood acknowledges funding from a NASA Astrobiology Postdoctoral Fellowship and an Australian Research Council DECRA (DE190100988).

Data availability statement

Data supporting the finding of this study are presented in this paper and in O'Connell et al., 2016 (an open source thesis). Additional data that support the findings of this study are available from the corresponding author upon request.

REFERENCES

Ainsworth, R.B. (2010) Prediction of stratigraphic compartmentalization in marginal marine reservoirs. In: Reservoir Compartmentalization (Eds Jolley, S.J., Fisher, Q.J., Ainsworth, R.B., Vrolijk, P.J. and Delisle, S.), Geological Society of London Special Publication, **347**, 199–218.

Ainsworth, R.B., Hasiotis, S.T., Amos, K.J., Krapf, C.B., Payenberg, T.H., Sandstrom, M.L., Vakarelov, B.K. and **Lang, S.C.** (2012) Tidal signatures in an intracratonic playa lake. Geology, **40**, 607-610.

Alexandersson, T. (1972) Intragranular growth of marine aragonite and Mg-calcite: evidence of precipitation from supersaturated seawater. Journal of Sedimentary Research, **42**, 441-460.

Bádenas, B., **Aurell, M.** and **Gasca, J.M.** (2018) Facies model of a mixed clastic–carbonate, wave-dominated open-coast tidal flat (Tithonian–Berriasian, north-east Spain). Sedimentology, **65**, 1631-1666.

Bučas, M., Sinkevičienė, Z., Kataržytė, M., Vaičiūtė, D., Petkuvienė, J., Stragauskaitė, V. and **Ilginė, R.** (2019) How much can the occurrence and coverage of charophytes in an estuarine lagoon (Curonian Lagoon) be explained by environmental factors? Estuarine, Coastal and Shelf Science, **216**, 128-138.

Boersma, J. and **Terwindt, J**. (1981) Neap–spring tide sequences of intertidal shoal deposits in a mesotidal estuary. Sedimentology, **28**, 151-170.

Booler, J. and **Tucker, M.E.** (2002) Distribution and geometry of facies and early diagenesis: the key to accommodation space variation and sequence stratigraphy: Upper Cretaceous Congost Carbonate platform, Spanish Pyrenees. Sedimentary Geology, **146**, 225-247.

Brachert, T., Forst, M., Pais, J., Legoinha, P. and **Reijmer, J.** (2003) Lowstand carbonates, highstand sandstones? Sedimentary Geology, **155**, 1-12.

Bray, N. (1988) Water mass formation in the Gulf of California. Journal of Geophysical Research: Oceans, **93**, 9223-9240.

Breda, A. and **Preto, N.** (2011) Anatomy of an Upper Triassic continental to marginal-marine system: the mixed siliciclastic–carbonate Travenanzes Formation (Dolomites, Northern Italy). Sedimentology, **58,** 1613-1647.

Bromley, R. (1996) Trace Fossils: biology, taphonomy and applications. Chapman and Hall, London, 361.

Bridge, J.S. (1993) Description and interpretation of fluvial deposits: a critical perspective. Sedimentology, **40**, 801-810.

Bright, J., Cohen, **A.S., Dettman, D.L.** and **Pearthree, P.A.** (2018a) Freshwater plumes and brackish lakes: Integrated microfossil and OC-Sr isotopic evidence from the late Miocene and early Pliocene Bouse Formation (California-Arizona) supports a lake overflow model for the integration of the lower Colorado River corridor. Geosphere, **14**, 1875-1911.

Bright, J., Cohen, A.S. and **Starratt, S.W.** (2018b) Distinguishing brackish lacustrine from brackish marine deposits in the stratigraphic record: A case study from the late Miocene and early Pliocene Bouse Formation, Arizona and California, USA. Earth-Science Reviews, **185**, 974-1003.

Bright, J., Cohen, A.S., Dettman, D.L., Pearthree, P.A., Dorsey, R.J. and **Homan, M.B.** (2016) Did a catastrophic lake spillover integrate the late Miocene early Pliocene Colorado River and the Gulf of California?: Microfaunal and stable isotope evidence from Blythe Basin, California-Arizona, USA. Palaios, **31**, 81-91.

Buising, A.V. (1990) The Bouse Formation and bracketing units, southeastern California and western Arizona: Implications for the evolution of the Proto-Gulf of California and the lower Colorado River. Journal of Geophysical Research: Solid Earth, **95**, 20111-20132.

Cadée, G.C. (2007) Balanuliths: Free-living clusters of the barnacle Balanus crenatus. Palaios, **22**, 680-681.

Castens-Seidell, B. (1984) Morphologies of Gypsum on a Modern Sabkha: Clues to Depositional Conditions. AAPG Bulletin, **68**, 460-460.

Castens-Seidell, B. and **Hardie, L.A.** (1984) Anatomy of a Modern Marine Sabkha in a Rift Valley Setting, Northwest Gulf of California, Baja California, Mexico. AAPG Bulletin, **68**, 460-460.

Chapin, C.E. (2008) Interplay of oceanographic and paleopalaeoclimate events with tectonism during middle to late Miocene sedimentation across the southwestern USA. Geosphere, **4**, 976-991.

Chiarella, D., Longhitano, S.G. and **Tropeano, M.** (2019) Different stacking patterns along an active fold-and-thrust belt—Acerenza Bay, Southern Apennines (Italy). Geology, **47**, 139-142.

Chiarella, D., Moretti, M., Longhitano, S.G. and **Muto, F.** (2016) Deformed cross-stratified deposits in the Early Pleistocene tidally-dominated Catanzaro strait-fill succession, Calabrian Arc (Southern Italy): Triggering mechanisms and environmental significance. Sedimentary Geology, **344**, 277-289.

Chiarella, D., Longhitano, S.G., Sabato, L. and **Tropeano, M.** (2012) Sedimentology and hydrodynamics of mixed (siliciclastic-bioclastic) shallow-marine deposits of Acerenza (Pliocene, Southern Apennines, Italy). Italian journal of geosciences, **131**, 136-151.

Chiarella, D. and **Longhitano, S.G.** (2012) Distinguishing Depositional Environments. In Shallow-Water Mixed, Bio-Siliciclastic Deposits On the Basis Of The Degree Of Heterolithic Segregation (Gelasian, Southern Italy). Journal of Sedimentary Research, **82**, 969-990.

Chiarella, D., Longhitano, S.G. and **Tropeano, M.** (2017) Types of mixing and heterogeneities in siliciclastic-carbonate sediments. Marine and Petroleum Geology, **88**, 617-627.

Choi, K.S. and **Dalrymple, R.W.** (2004) Recurring tide-dominated sedimentation in Kyonggi Bay (west coast of Korea): similarity of tidal deposits in late Pleistocene and Holocene sequences. Marine Geology, **212**, 81-96.

Coueffe, R., Tessier, B., Gigot, P. and **Beaudoin, B.** (2004) Tidal Rhythmites as Possible Indicators of Very Rapid Subsidence in a Foreland Basin: An Example from the Miocene Marine

Molasse Formation of the Digne Foreland Basin, SE France. Journal of Sedimentary Research **74**, 746-759.

Crossey, L.C., Karlstrom, K.E., Dorsey, R., Pearce, J., Wan, E., Beard, L.S., Asmerom, Y., Polyak, V., Crow, R.S., Cohen, A., Bright, J. and **Pecha, M.E.** (2015) Importance of groundwater in propagating downward integration of the 6-5 Ma Colorado River system: Geochemistry of springs, travertines, and lacustrine carbonates of the Grand Canyon region over the past 12 Ma. Geosphere, **11**, 660-682.

Crossey, L.C., Karlstrom K.E., Crow R.S., Ferguson, C., and **Dorsey, R.J.** (2017) Towards a depositional model for travertines of the Bouse Formation: examples from the southern Blythe Basin. *In:* Reynolds, R.E. (Ed.), 2017 Desert Symposium Field Guide and Proceedings, California State University Desert Studies Center, Zzyzx, CA, p. 174-179.

Dalrymple, R., Kurcinka, C., Jablonski, B., Ichaso, A. and **Mackay, D.** (2015) Deciphering the relative importance of fluvial and tidal processes in the fluvial–marine transition. In: Developments in Sedimentology, **68**, pp. 3-45. Elsevier.

Dalrymple, R.W. (2010) Tidal depositional systems. In: Facies Models (Eds N.P. James and R.W. Dalrymple), Geological Association of Canada, **4**, 201– 231.

Dalrymple, R.W., Makino, Y. and **Zaitlin, B.A.** (1991) Temporal and spatial patterns of rhythmite deposition on mud flats in the macrotidal Cobequid Baya Salmon river estuary, Bay of Fundy, Canada. In: Clastic Tidal Sedimentology (Eds D.G. Smith, G.E. Reinson, B.A. Zaitlin and R.A. Rahmani), **16,** pp. 137–160. Canadian Society Petroleum Geologists Memories.

Dalrymple, R.W. and Rhodes, R.N. (1995) Estuarine dunes and bars. In: Geomorphology and sedimentology of estuaries (Ed. G.M.E. Perillo), **53**, pp. 359– 422. Elsevier, Amsterdam.

Dashtgard, S.E. and Gingras, M.K. (2005) Facies architecture and ichnology of recent salt-marsh deposits: Waterside Marsh, New Brunswick, Canada. Journal of Sedimentary Research, **75**, 596-607.

Dashtgard, S.E. and **La Croix, A.D.** (2015) Sedimentological trends across the tidal–fluvial transition, Fraser River, Canada: a review and some broader implications. In: Fluvial-Tidal Sedimentology (Eds P.J. Ashworth, J.L. Best, D.R. Parsons), **68**, pp. 111-126. Elsevier.

Davis, R.A.J. (2012) Tidal signatures and their preservation potential in stratigraphic sequences. In: Principles of Tidal Sedimentology (Eds R.W. Dalrymple and R.A.J. Davis), pp. 35– 55. Springer, New York.

Di Stefano, A. and **Longhitano, S.G.** (2009) Tectonics and sedimentation of the Lower and Middle Pleistocene mixed siliciclastic/bioclastic sedimentary successions of the Ionian Peloritani Mts (NE Sicily, Southern Italy): the onset of opening of the Messina Strait. Central European Journal of Geosciences, **1**, 33-62.

Dolan, J.F. (1989) Eustatic and tectonic controls on deposition of hybrid siliciclastic/carbonate basinal cycles: discussion with examples. AAPG Bulletin, **73**, 1233-1246.

Dorsey, R.J. and **Kidwell, S.M.** (1999) Mixed carbonate-siliciclastic sedimentation on a tectonically active margin: Example from the Pliocene of Baja California Sur, Mexico. Geology, **27**, 935-938.

Dorsey, R.J., O'Connell, B., McDougall, K. and **Homan, M.B.** (2018) Punctuated sediment discharge during early Pliocene birth of the Colorado River: Evidence from regional stratigraphy, sedimentology, and paleontology. Sedimentary Geology. **363**, 1-33.

Dorsey, R.J., O'Connell, B., Homan, M., and **Bennett, S.E.K.,** (2017) Influence of the Eastern California Shear Zone on deposition of the Mio-Pliocene Bouse Formation: Insights from the Cibola area, Arizona. In: Desert Symposium Field Guide and Proceedings (Ed. Reynolds, R.E.) pp. 150-157.

Droser, M.L. and **Bottjer, D.J.** (1986) A semiquantitative field classification of ichnofabric. Journal of Sedimentary Research, **56**, 558-559.

Ezcurra, E. and **Rodrigues, V.** (1986) Rainfall patterns in the Gran Desierto, Sonora, Mexico. Journal of Arid Environments, **10**, 13-28.

Faulds, J.E., Schreiber, B.C., Langenheim, V.E., Hinz, N.H., Shaw, T.H., Heizler, M.T., Perkins, M.E., El Tabakh, M. and **Kunk, M.J.** (2016) Paleogeographic implications of late Miocene lacustrine and nonmarine evaporite deposits in the Lake Mead region: Immediate precursors to the Colorado River. Geosphere, **12**, 721-767.

Flaig, P.P., Hasiotis, S.T., Prather, T.J. and **Burton, D.** (2019) Characteristics of a Campanian delta deposit controlled by alternating river floods and tides: the Loyd Sandstone, Rangely Anticline, Colorado, USA. Journal of Sedimentary Research, **89**, 1181-1206.
Flügel, E. (2004) Microfacies Analysis of Carbonate Rocks. Analysis, Interpretation and Application, p. 976. SpringerVerlag, Berlin.

Folk, R.L. (1974) The natural history of crystalline calcium carbonate; effect of magnesium content and salinity. Journal of Sedimentary Research, **44**, 40-53.

Forrester, R. (1991) Pliocene-climate history of the western United States derived from lacustrine ostracods. Quaternary Science Reviews, **10**, 133-146

Foster, M., Riosmena-Rodriguez, R., Steller, D.L. and **Woelkerling, W.J.** (1997) Living rhodolith beds in the Gulf of California and their implications. Pliocene carbonates and related facies flanking the Gulf of California, Baja California, Mexico. Geological Society of America Special Paper, **318**, 127-139.

Gardner, K., and, **Dorsey, R.J.,** (in press). Mixed carbonate-siliciclastic sedimentation at the margin of a late Miocene tidal strait, lower Colorado River Valley, southwestern USA. Sedimentology (accepted with minor revisions November 11, 2020).

Gingras, M.K. and **MacEachern, J.A.** (2012) Tidal ichnology of shallow-water clastic settings. In: Principles of Tidal Sedimentology (Eds R.W. Dalrymple and R.A.J. Davis), pp. 57-77. Springer.

Gingras, M.K., MacEachern, J.A. and **Dashtgard, S.E.** (2012) The potential of trace fossils as tidal indicators in bays and estuaries. Sedimentary Geology, **279**, 97-106.

Gingras, M.K., Pemberton, S.G., Saunders, T. and **Clifton, H.E.** (1999) The Ichnology of Modern and Pleistocene Brackish-Water Deposits at Willapa Bay, Washington: Variability in Estuarine Settings. **14**, 352.

Ginsburg, R.N (1971). Landward movement of carbonate mud: new model for regressive cycles in carbonates. AAPG Bulletin, **55**, 340-340.

Glenn, E.P., Nagler, P.L., Brusca, R.C. and **Hinojosa-Huerta, O.** (2006) Coastal wetlands of the northern Gulf of California: inventory and conservation status. Aquatic Conservation: Marine and Freshwater Ecosystems, **16**, 5-28.

Gootee, B.F., Pearthree, P.A., House, P.K., Youberg, A., Spencer, J.E., and **O'Connell, B.** (2016) Geologic map of the Cibola 7 ½' Quadrangle and the northwestern part of Cibola SE 7 ½' Quadrangle, La Paz County, Arizona, and Imperial County, California. Arizona Geological Survey Digital Map DGM-117, scale 1:24,000, with text.

Halfar, J., Ingle Jr, J.C. and **Godinez-Orta, L.** (2004) Modern non-tropical mixed carbonate-siliciclastic sediments and environments of the southwestern Gulf of California, Mexico. Sedimentary Geology, **165**, 93-115.

Halfar, J., Strasser, M., Riegl, B. and **Godinez-Orta, L.** (2006) Oceanography, sedimentology and acoustic mapping of a bryomol carbonate factory in the northern Gulf of California, Mexico. Geological Society, London, Special Publications, **255**, 197-215.

Hammersburg, S.R., Hasiotis, S.T. and **Robison, R.A**. (2018) Ichnotaxonomy of the Cambrian Spence Shale Member of the Langston Formation, Wellsville Mountains, Northern Utah, USA. Paleontological Contributions, **20**, 1-66.

Häntzschel, W. (1975) Treatise on Invertebrate Paleontology: Miscellanea: Trace Fossils and Problematica. Pt. W. Suppl. 1. Geological Society of America.

Hardie, L.A. (1977) Sedimentation on the Modern Carbonate Tidal Flats of Northwest Andros Island, Bahamas: The Johns Hopkins University Studies in Geology. The Johns Hopkins University Press, Baltimore.

Hasiotis, S. (2002) Continental Trace Fossils: SEPM Short Course Notes, no. 51. Tulsa, Oklahoma, 134.

Hasiotis, S.T. and **Mitchell, C.E.** (1993) A comparison of crayfish burrow morphologies: Triassic and Holocene fossil, paleo-and neo-ichnological evidence, and the identification of their burrowing signatures. Ichnos: An International Journal of Plant & Animal, **2**, 291-314.

Hasiotis, S., McPherson, J. and **Reilly, M.** (2013) Using ichnofossils to reconstruct the depositional history of sedimentary successions in alluvial, coastal-plain, and deltaic settings. In: IPTC 2013: International Petroleum Technology Conference, pp. cp-350-00442. European Association of Geoscientists & Engineers.

Hauck, T.E., Dashtgard, S.E., Pemberton, S.G. and **Gingras, M.K.** (2009) Brackish-water ichnological trends in a microtidal barrier island-embayment system, Kouchibouguac National Park, New Brunswick, Canada. Palaios, **24**, 487–496.

Homan, M.B. (2014) Sedimentology and Stratigraphy of the Miocene-Pliocene Bouse Formation near Cibola, Arizona and Milpitas Wash, California: Implications for the Early Evolution of the Colorado River, Thesis University of Oregon.

House, P.K., Pearthree, P.A. and **Perkins, M.E.** (2008) Stratigraphic evidence for the role of lake spillover in the inception of the lower Colorado River in southern Nevada and western Arizona. Geological Society of America Special Papers, **439**, 335-353.

Howard, K.A., House, P.K., Dorsey, R.J. and **Pearthree, P.A.** (2015) River-evolution and tectonic implications of a major Pliocene aggradation on the lower Colorado River: The Bullhead Alluvium. Geosphere, **11**, 1-30.

Ibarra, D.E., Oster, J.L., Winnick, M.J., Caves Rugenstein, J.K., Byrne, M.P. and **Chamberlain, C.P.** (2018) Warm and cold wet states in the western United States during the Pliocene–Pleistocene. Geology, **46**, 355-358.

Jackson, A.M., Hasiotis, S.T. and **Flaig, P.P.** (2016) Ichnology of a paleopolar, river-dominated, shallow marine deltaic succession in the Mackellar Sea: the Mackellar Formation (Lower Permian), central Transantarctic Mountains, Antarctica. Palaeogeography, Palaeoclimatology, Palaeoecology, **441**, 266-291.

James, N.P. (1979) Shallowing-upward sequences in carbonates, In Facies Models (Ed R.G. Walker) Canadian Journal of Geosciences, pp. 108-119.

James, N.P. (1997) The cool-water carbonate depositional realm. In Cool-water Carbonates (Eds. N.P. James and J.A.D. Clarke, SEPM Special Publication, **56**, 1–20.

James, N.P. and **Lukasik, J.** (2010) Cool-and cold-water neritic carbonates. In Facies models, 4 (Eds. R.W. Dalrymple and N.P. James) Geological Association of Canada, pp. 371–399.

Kearney, W.S. and **Fagherazzi, S.** (2016) Salt marsh vegetation promotes efficient tidal channel networks. Nature Communications, **7**, 12287.

Klein, G.D. (1970) Depositional and dispersal dynamics of intertidal sand bars. Journal of Sedimentary Research, **40**, 1095-1127.

Klein, G.D. (1977) Clastic tidal facies: Champaign, Illinois. Continuing Education Publication Company, 149.

Kurcinka, C., Dalrymple, R.W. and **Gugliotta, M.** (2018) Facies and architecture of river-dominated to tide-influenced mouth bars in the lower Lajas Formation (Jurassic), Argentina. AAPG Bulletin, **102**, 885-912.

Kvale, E.P., Bowie, C.M., Flenthrope, C., Mace, C., Parrish, J.M., Price, B., Anderson, S. and **DiMichele, W.A.** (2019) Facies variability within a mixed carbonate-siliciclastic sea-floor fan (upper Wolfcamp Fm., Permian, Delaware Basin, New Mexico). AAPG Bulletin, **104**, 525-563.

La Croix, A.D., Dashtgard, S.E., Gingras, M.K., Hauck, T.E. and **MacEachern, J.A.** (2015) Bioturbation trends across the freshwater to brackish-water transition in rivers. Palaeogeography, Palaeoclimatology, Palaeoecology, **440**, 66-77.

Lavín, M. and **Marinone, S.** (2003) An overview of the physical oceanography of the Gulf of California. In: Nonlinear processes in geophysical fluid dynamics (Eds. O. Fuentes, J. Sheinbaum, and J. Torre) pp. 173-204. Springer.

Lavín, M., Godınez, V. and **Alvarez, L. (**1998) Inverse-estuarine features of the Upper Gulf of California. Estuarine, Coastal and Shelf Science, **47**, 769-795.

Li, M.Z., Shaw, J., Todd, B.J., Kostylev, V.E. and **Wu, Y.** (2014) Sediment transport and development of banner banks and sandwaves in an extreme tidal system: Upper Bay of Fundy, Canada. Continental Shelf Research, **83**, 86-107.

Lokier, S.W., Knaf, A. and Kimiagar, S. (2013) A quantitative analysis of Recent arid coastal sedimentary facies from the Arabian Gulf Coastline of Abu Dhabi, United Arab Emirates. Marine Geology, **346**, 141-152.

Longhitano, S.G. (2011) The record of tidal cycles in mixed silici–bioclastic deposits: examples from small Plio–Pleistocene peripheral basins of the microtidal Central Mediterranean Sea. Sedimentology, **58**, 691-719.

Longhitano, S.G., Chiarella, D., Di Stefano, A., Messina, C., Sabato, L. and Tropeano, M. (2012a) Tidal signatures in Neogene to Quaternary mixed deposits of southern Italy straits and bays. Sedimentary Geology, **279**, 74-96.

Longhitano, S.G., Mellere, D., Steel, R.J. and Ainsworth, R.B. (2012b) Tidal depositional systems in the rock record: A review and new insights. Sedimentary Geology, **279**, 2-22.

Longhitano, S.G., Chiarella, D. and **Muto, F.** (2014) Three-dimensional to two-dimensional cross-strata transition in the lower Pleistocene Catanzaro tidal strait transgressive succession (southern Italy). Sedimentology, **61**, 2136-2171.

Longhitano, S.G. and **Nemec, W.** (2005) Statistical analysis of bed-thickness variation in a Tortonian succession of biocalcarenitic tidal dunes, Amantea Basin, Calabria, southern Italy. Sedimentary Geology, **179**, 195-224.

Longhitano, S.G., Sabato, L., Tropeano, M. and **Gallicchio, S.** (2010) A mixed bioclastic–siliciclastic flood-tidal delta in a micro tidal setting: depositional architectures and hierarchical internal organization (Pliocene, Southern Apennine, Italy). Journal of Sedimentary Research, **80**, 36-53.

MacEachern, J.A., Bann, K.L., Gingras, M.K., and **Pemberton, S.G.,** (2007) Applied Ichnology: SEPM, Short Course Notes 52, 380.

Marinone, S.G. (1997) Tidal residual currents in the Gulf of California: Is the M2 tidal constituent sufficient to induce them?. Journal of Geophysical Research. Oceans, **102**, 8611-8623.

McDougall, K. and **Martínez, A.Y.M.** (2014) Evidence for a marine incursion along the lower Colorado River corridor. Geosphere, **10**, 842-869.

McDougall, K., Reheis, M., Hershler, R. and **Miller, D.** (2008) Late Neogene marine incursions and the ancestral Gulf of California. Special Papers-Geological Society of America, **439**, 355-373.

McNeill, D.F., Cunningham, K.J., Guertin, L.A., and **Anselmetti, F.S.** (2004) Depositional themes of mixed carbonate-siliciclastics in the South Florida Neogene: application to ancient deposits. In: Integration of Outcrop and Modern Analogues in Reservoir Modeling (Eds G.M. Grammer, P.M. Harris, G.P. Eberli,) AAPG Memoir 80, 23–43.

Meng, X., Ge, M. and **Tucker, M.E.** (1997) Sequence Sequence stratigraphy, sea-level changes and depositional systems in the Cambro-Ordovician of the North China carbonate platform. Sedimentary Geology, **114**, 189-222.

Metzger, D.G., Loeltz, O.J. and **Irelan, B**. 1973. Geohydrology of the Parker-Blythe-Cibola area, Arizona and California. 2330-7102.

Metzger, D. (1968) The Bouse Formation (Pliocene) of the Parker-Blythe-Cibola area, Arizona and California. US Geological Survey Professional Paper, **600**, D126-D136.

Miller, D.M., Reynolds, R.E., Bright, J.E. and **Starratt, S.W**. (2014) Bouse formation in the Bristol basin near Amboy, California, USA. Geosphere, **10**, 462-475.

Molnar, P. and **Cane, M.A.** (2007) Early Pliocene (pre–Ice Age) El Niño–like global climate: Which El Niño? Geosphere, **3**, 337-365.

Michel, J., Borgomano, J., and **Reijmer, J.J.** (2018) Heterozoan carbonates: When, where and why? A synthesis on parameters controlling carbonate production and occurrences. Earth-Science Reviews, **182**, 50-67.

Morzaria-Luna, H.N., Castillo-López, A., Danemann, G.D. and **Turk-Boyer, P.** (2014) Conservation strategies for coastal wetlands in the Gulf of California, Mexico. **22**, 267-288.

Mount, J. (1985) Mixed siliciclastic and carbonate sediments: a proposed first-order textural and compositional classification. Sedimentology, **32**, 435-442.

Mount, J.F. (1984) Mixing of siliciclastic and carbonate sediments in shallow shelf environments. Geology, **12**, 432-435.

Nio, S.D., and **Yang, C.S.** (1991). Diagnostic attributes of clastic deposits: a review. In: Clastic Tidal Sedimentology (Eds D.G. Smith, G.E. Reinson, B.A. Zaitlin and R.A. Rahmani), **16**, pp 3-28, Canadian Society Petroleum Geologists Memories.

Norris, J.N. (2010). Marine algae of the Northern Gulf of California: Chlorophyta and Phaeophyceae. Smithsonian contributions to botany. **94**, 1–276

Nyman, J.A., DeLaune, R.D., Roberts, H.H. and **Patrick Jr, W**. (1993) Relationship between vegetation and soil formation in a rapidly submerging coastal marsh. Marine Ecology Progress Series, 269-279.

O'Connell, B., Dorsey, R.J. and **Humphreys, E.D.** (2017) Tidal rhythmites in the southern Bouse Formation as evidence for post-Miocene uplift of the lower Colorado River corridor. Geology, **45**, 99-102.

O'Connell, B. (2016). Sedimentology and depositional history of the Miocene–Pliocene southern Bouse Formation, Arizona and California. M.S. thesis, University of Oregon, Eugene, Oregon, 148 p.

Overstreet, R.B., Oboh-Ikuenobe, F.E. and **Gregg, J.M.** (2003) Sequence stratigraphy and depositional facies of Lower Ordovician cyclic carbonate rocks, southern Missouri, USA. Journal of Sedimentary Research, **73**, 421-433.

Page, M.C. and **Dickens, G.R.** (2005) Sediment fluxes to Marion Plateau (southern Great Barrier Reef province) over the last 130 ky: new constraints on 'transgressive-shedding'off northeastern Australia. Marine Geology, **219**, 27-45.

Pemberton, S.G., Flach, P.D. and **Mossop, G.D.** (1982) Trace fossils from the Athabasca oil sands, Alberta, Canada. Science, **217**, 825-827.

Pemberton, S.G. and **Wightman, D.M.** (1992) Ichnological characteristics of brackish water deposits. In: Applications of Ichnology to Petroleum Exploration (Ed. S.G. Pemberton), SEPM Core Workshop, **17**, 141–167.

Pemberton, S.G. (2001) Ichnology & sedimentology of shallow to marginal marine systems. Geol. Assoc. Can., Short Course, **15**, 343.

Pilkey, O., Bush, D.M. and **Rodríguez, R.W.** (1988) Carbonate-terrigenous sedimentation on the north Puerto Rico shelf. In: Carbonate–Clastic Transitions (Eds. L.J. Doyle, H.H. Roberts), 42, pp. 231-250. Elsevier.

Piller, W.E. and **Mansour, A.M.** (1994) Origin and transport mechanisms of non-carbonate sediments in a carbonate-dominated environment (Northern Safaga Bay, Red Sea, Egypt). Abh Geol Bundesanstalt, **50**, 369–379

Postma, G. (1990) An analysis of the variation in delta architecture. Terra Nova, **2**, 124-130.

Pugh, D. (1987) Tides, surges and mean sea-level: a handbook for engineers and scientists. John Wiley, Chichester, UK. 472 pp.

Purser, B.H. (1973) The Persian Gulf: Holocene carbonate sedimentation and diagenesis in a shallow epicontinental sea. Springer-Verlag, New York, Heidelberg, Berlin, 471 pp.

Rankey, E.C. and Berkeley, A. (2012) Holocene carbonate tidal flats. In: Principles of Tidal Sedimentology (Eds R.W. Dalrymple and R.A.J. Davis), pp. 507-535. Springer.

Remeika, P., Fischbein, I.W. and **Fischbein, S.A.** (1988) Lower Pliocene petrified wood from the Palm Spring Formation, Anza Borrego Desert State Park, California. Review of palaeobotany and palynology, **56**, 183-198.

Richard, S.M. (1993) Palinspastic reconstruction of southeastern California and southwestern Arizona for the middle Miocene. Tectonics, **12**, 830-854.

Romano, M. and **Whyte, M.** (2015) A review of the trace fossil Selenichnites. Proceedings of the Yorkshire Geological Society, **60**, 275-288.

Roskowski, J.A., Patchett, P.J., Spencer, J.E., Pearthree, P.A., Dettman, D.L., Faulds, J.E. and **Reynolds, A.C**. (2010) A late Miocene–early Pliocene chain of lakes fed by the Colorado River: Evidence from Sr, C, and O isotopes of the Bouse Formation and related units between Grand Canyon and the Gulf of California. GSA Bulletin, **122**, 1625-1636.

Rubin, D.M. (2012) A unifying model for planform straightness of ripples and dunes in air and water. Earth-science Reviews, **113**, 176-185.

Rubin, D.M. and **Friedman, G.M.** (1977) Intermittently emergent shelf carbonates: an example from the Cambro-Ordovician of eastern New York State. Sedimentary Geology, **19**, 81-106.

Salzmann, U., Williams, M., Haywood, A.M., Johnson, A.L., Kender, S. and **Zalasiewicz, J.** (2011) Climate and environment of a Pliocene warm world. Palaeogeography, Palaeoclimatology, Palaeoecology, **309**, 1-8.

Sanders, D. and **Höfling, R.** (2000) Carbonate deposition in mixed siliciclastic–carbonate environments on top of an orogenic wedge (Late Cretaceous, Northern Calcareous Alps, Austria). Sedimentary Geology, **137**, 127-146.

Sarjeant, W., Reynolds, R. and **Kissell-Jones, M.** (2002) Fossil creodont and carnivore footprints from California, Nevada, and Wyoming. Between the Basins: Exploring the Western Mojave and Southern Basin and Range Province. Fullerton, California State University, Desert Studies Consortium, 37-50.

Sarjeant, W.A. and **Reynolds, R.** (2001) Bird footprints from the Miocene of California. In: The changing face of the east Mojave Desert: abstracts from the 2001 Desert Symposium, pp. 21-40.

Schwarz, E., Veiga, G.D., Álvarez Trentini, G., Isla, M.F. and **Spalletti, L.A.** (2018) Expanding the spectrum of shallow-marine, mixed carbonate–siliciclastic systems: Processes, facies distribution and depositional controls of a siliciclastic-dominated example. Sedimentology, **65**, 1558-1589.

Sherrod, D.R. and **Tosdal, R.M.** (1991) Geologic setting and Tertiary structural evolution of southwestern Arizona and southeastern California. Journal of Geophysical Research: Solid Earth, **96**, 12407-12423.

Shinn, E.A. (1983) Tidal flat environment. In: Carbonate depositional environments, AAPG Memoir, **33**, 171-210.

Shinn, E.A. and **Ginsburg, R.** (1964) Formation of Recent dolomite in Florida and the Bahamas. AAPG Bulletin, **48**, 547-547.

Smith, P.B. (1970) New evidence for a Pliocene marine embayment along the lower Colorado River area, California and Arizona. Geological Society of America Bulletin, **81**, 1411-1420.

Spencer, J.E., Pearthree, P.A., House, P.K., Reheis, M., Hershler, R. and **Miller, D.** (2008) An evaluation of the evolution of the latest Miocene to earliest Pliocene Bouse lake system in the lower Colorado River valley, southwestern USA. Special Papers Geological Society of America, **439**, 375.

Spencer, J.E. and **Jonathan Patchett, P.** (1997) Sr isotope evidence for a lacustrine origin for the upper Miocene to Pliocene Bouse Formation, lower Colorado River trough, and implications for timing of Colorado Plateau uplift. Geological Society of America Bulletin, **109**, 767-778.

Spencer, J.E., Patchett, P.J., Pearthree, P.A., House, P.K., Sarna-Wojcicki, A.M., Wan, E., Roskowski, J.A. and **Faulds, J.E.** (2013) Review and analysis of the age and origin of the Pliocene Bouse Formation, lower Colorado River Valley, southwestern USA. Geosphere, **9**, 444-459.

Steinhardt, T., Karez, R., Selig, U. and **Schubert, H**. (2009) The German procedure for the assessment of ecological status in relation to the biological quality element "Macroalgae & Angiosperms" pursuant to the European Water Framework Directive (WFD) for inner coastal waters of the Baltic Sea. Rostocker Meeresbiologische Beiträge, **22**, 42.

Sztano, O. and **de Boer, P.L.** (1995) Basin dimensions and morphology as controls on amplification of tidal motions (the Early Miocene North Hungarian Bay). Sedimentology, **42**, 665-682.

Tape, C.H., Cowan, C.A. and **Runkel, A.C.** (2003) Tidal-bundle sequences in the Jordan Sandstone (Upper Cambrian), southeastern Minnesota, USA: evidence for tides along inboard shorelines of the Sauk epicontinental sea. Journal of Sedimentary Research, **73**, 354-366.

Tcherepanov, E.N., Droxler, A.W., Lapointe, P., Dickens, G.R., Bentley, S.J., Beaufort, L., Peterson, L.C., Daniell, J. and **Opdyke, B.N.** (2008) Neogene evolution of the mixed carbonate-siliciclastic system in the Gulf of Papua, Papua New Guinea. Journal of Geophysical Research: Earth Surface, **113**, F01S21.

Thompson, R.S. and Fleming, R.F. (1996) Middle Pliocene vegetation: reconstructions, paleoclimatic inferences, and boundary conditions for climate modeling. Marine Micropaleontology, **27**, 27-49.

Thompson, R.S. (1991) Pliocene environments and climates in the western United States. Quaternary Science Reviews, **10**, 115-132.

Thompson, R.W. (1975) Tidal-flat sediments of the Colorado River delta, northwestern Gulf of California. In: Tidal Deposits (Ed R.N. Ginsburg), pp. 57-65. Springer.

Todd, B.J., Shaw, J., Li, M.Z., Kostylev, V.E. and **Wu, Y.** (2014) Distribution of subtidal sedimentary bedforms in a macrotidal setting: The Bay of Fundy, Atlantic Canada. Continental Shelf Research, **83**, 64-85.

Turak, J. (2000) Re-evaluation of the Miocene. Pliocene depositional history of the Bouse Formation, Colorado River trough, southern Basin and Range (CA, NV, and AZ). MS thesis, Laramie, University of Wyoming.

Umhoefer, P.J., Darin, M.H., Bennett, S.E., Skinner, L.A., Dorsey, R.J. and **Oskin, M.E.** (2018) Breaching of strike-slip faults and successive flooding of pull-apart basins to form the Gulf of California seaway from ca. 8–6 Ma. Geology, **46**, 695-698.

Van Siclen, D.C. (1958) Depositional topography—examples and theory. AAPG Bulletin, **42**, 1897-1913.

Wilson, J.L. (1967) Cyclic and reciprocal sedimentation in Virgilian strata of southern New Mexico. Geological Society of America Bulletin, **78**, 805-818.

Winnick, M.J., Welker, J.M., and **Chamberlain, C.P.** (2013) Stable isotopic evidence of El Nio–like atmospheric circulation in the Pliocene western United States: Climate of the Past, **9**, 903–912.

Wright, V. (1984) Peritidal carbonate facies models: a review. Geological Journal, **19**, 309-325.

Zeller, M., Verwer, K., Eberli, G.P., Massaferro, J.L., Schwarz, E. and **Spalletti, L.** (2015) Depositional controls on mixed carbonate–siliciclastic cycles and sequences on gently inclined shelf profiles. Sedimentology, **62**, 2009-2037.

Zullo, V. and Buising, A. (1989) An unusual species of the Balanus amphitrite Darwin complex (Cirripedia, Balanidea) from the ancestral Colorado river delta in western Arizona and southeastern California. Proceedings of the Biological Society of Washington, **102**, 924-932.

Zuffa, G.G. (1980) Hybrid arenites; their composition and classification. Journal of Sedimentary Research, **50**, 21-29.